ISAS - INTERNATIONAL SCHOOL FOR ADVANCED STUDIES

SISSA ISAS

SCUOLA INTERNAZIONALE SUPERIORE DI STUDI AVANZATI
INTERNATIONAL SCHOOL FOR ADVANCED STUDIES

Electron-Vibron Interaction, Berry Phase and Superconductivity in Charged Buckminsterfullerene

Thesis submitted for the degree of

"Magister Philosophiae"

CANDIDATE

Nicola Manini

SUPERVISOR

Prof. Erio Tosatti

October 1993

TRIESTE

SISSA - SCUOLA INTERNAZIONALE SUPERIORE STUDI AVANZATI
TRIESTE
Strada Costiera 11

Electron–Vibron Interactions and Berry Phases in Charged Buckminsterfullerene: Part I

Assa Auerbach*
Physics Department, Technion, Haifa, Israel,
Nicola Manini[a†] and Erio Tosatti[a,b‡]
a) International School for Advanced Studies (SISSA), via Beirut 2-4, I-34013 Trieste, Italy.
b) International Centre for Theoretical Physics (ICTP), P.O. BOX 586, I-34014 Trieste, Italy.

January 12, 1994

Abstract

A simple model for electron-vibron interactions on charged buckminsterfullerene $C_{60}{}^{n-}$, $n = 1, \ldots 5$, is solved both at weak and strong couplings. We consider a single H_g vibrational multiplet interacting with t_{1u} electrons. At strong coupling the semiclassical dynamical Jahn-Teller theory is valid. The Jahn-Teller distortions are unimodal for n=1,2,4,5 electrons, and bimodal for 3 electrons. The distortions are quantized as rigid body pseudo–rotators which are subject to geometrical Berry phases. These impose ground state degeneracies and dramatically change zero point energies. Exact diagonalization shows that the semiclassical level degeneracies and ordering survive well into

*Email: assa@phassa.technion.ac.il
†Email: manini@tsmi19.sissa.it
‡Email: tosatti@tsmi19.sissa.it

SISSA REF: 4/94/CM/MB

the weak coupling regime. At weak coupling, we discover an enhancement factor of 5/2 for the pair binding energies over their classical values. This has potentially important implications for superconductivity in fullerides, and demonstrates the shortcoming of Migdal–Eliashberg theory for molecular crystals.

PACS: 31.30,33.10.Lb,71.38.+i,74.20.-z,74.70.W

1 Introduction

The soccer-ball shaped molecule C_{60} (buckminsterfullerene) and its various crystalline compounds have ignited enormous interest in the chemistry and physics community in past two years [1]. C_{60} is a truncated icosahedron. From a physicist's standpoint, the charged molecule is fundamentally interesting, because the high molecular symmetry gives rise to degeneracies in both electronic and vibrational systems. Thus, the molecule is very sensitive to perturbations. In particular, electron–phonon and electron–electron interactions are expected to produce highly correlated ground states and excitations.

Superconductivity has been discovered in alkali doped buckminsterfullerenes A_3C_{60} (A=K,Cs,Rb), with relatively high transition temperatures ($T_c \approx 20°$–$30° K$). There are experimental indications that the pairing mechanism originates in the electronic properties of a single molecule. The pair binding energy is a balance of electron-vibron interactions [2, 3, 4] and electron-electron interactions [5]. The relative contributions and signs of the two interactions is under some controversy.

The electron–vibron school has identified certain five-fold degenerate H_g (d-wave like) vibrational modes which couple strongly to the t_{1u} Lowest Unoccupied Molecular Orbital (LUMO) [2, 3, 4, 6]. Varma, Zaanen and Raghavachari [2] as well as Schluter *et al* and, more recently, Antropov *et al* proposed that these modes undergo a Jahn-Teller (JT) distortion and calculated the

induced pair binding energies at several fillings. They used the *classical approximation*, and restricted their calculation to unimodal distortions (defined later). The general conclusion of this approach is that, while the calculated λ is sizeable, one still requires a large reduction of the Coulomb pseudo–potential μ^* in order to explain the highest transition temperatures. On the other hand, Gunnarsson *et al* independently estimate a large $\mu^* \approx 0.4$, i.e. there is no mechanism providing such a reduction.

However, estimates of the electron–vibron coupling constant g do not justify the classical JT approximation. C_{60} is estimated by frozen phonon calculations to be in the weak coupling regime $g \leq 1$ where quantum corrections are important.

In this paper (Part I) we study the isolated C_{60}^{n-} charged molecule. In particular, we shall reconsider the same JT model, but diagonalize the quantum Hamiltonian for the full range of the coupling constant. We shall find that quantum corrections to the classical JT theory introduce novel qualitative features, and are quantitatively important for the pair binding energies.

The quantum fluctuations involve interference effects due to geometrical Berry phases. Berry phases appear in a wide host of physical phenomena [7, 8]. Here we find it in the context of a "Molecular Aharonov-Bohm (MAB) effect", originally discovered by Longuet-Higgins [9]. The MAB effect has important consequences on the vibron spectrum. For example, it produces half–odd integer quantum numbers in the spectrum of triangular molecules [9, 7], an effect recently confirmed spectroscopically in Na_3 [10]. This kind of Berry phase is important also in scattering of hydrogen molecules [11]. Recently, it has been suggested that a geometrical Berry phase may be relevant in fullerene ions [12, 13, 14]. Here we show that Berry phases produce *selection rules* for the pseudo–rotational quantum numbers and *kinematical* restrictions which effect the pairing interaction between electrons. Although the semiclassical and Berry phase description is appropriate in strong coupling, the level ordering and degeneracies are found to survive for arbitrary

coupling, particularly in the weak coupling regime, which is closer to actual C_{60}. For this reason we devote a large portion of this paper to the semiclassical theory, which helps to build physical intuition for further extensions of the model.

This paper is organized as follows: In Section 2 the basic model is introduced. Section 3 calculates the JT distortions in the classical limit. Section 4 derives the semiclassical quantization about the JT manifold. The geometrical Berry phases are calculated, and their effect on the semiclassical spectrum is obtained up to order g^{-2}. Section 5 describes the exact diagonalization results, and compares them to the semiclassical theory, and to weak coupling perturbation theory. The pair binding energies are determined in Section 6. In Section 7 we summarize the paper and discuss our main result: that the effective pair binding energies are larger by a factor of 3 than the pair interaction energy in Migdal–Eliashberg's theory. In a following paper [15] we shall extend the model to all A_g and H_g modes with realistic physical parameters. This will allow us to explore the experimental consequences of the electron–vibron interactions.

2 The Electron–Vibron Model

The single electron LUMO states of C_{60} are in a triplet of t_{1u} representation. We consider the H_g (five dimensional) vibrational multiplet which couples to these electrons. t_{1u} and H_g are the icosahedral group counterparts of the spherical harmonics $\{Y_{1m}\}_{m=-1}^{1}$, and $\{Y_{2M}\}_{M=-2}^{2}$ respectively. By replacing the truncated icosahedron (soccer ball) symmetry group by the spherical group, we ignore lattice corrugation effects. These are expected to be small since they do not lift the degeneracies of the $L = 1, 2$ representations.

The Hamiltonian is thus defined as

$$H = H^0 + H^{e-v} , \tag{1}$$

where,

$$H^0 = \hbar\omega \sum_{MI} \left(b^\dagger_{MI} b_{MI} + \frac{1}{2} \right) + (\epsilon - \mu) \sum_{ms} c^\dagger_{ms} c_{ms} \ . \tag{2}$$

$b^\dagger_{MI}$ creates a vibron with azimuthal quantum number M, and $c^\dagger_{ms}$ creates an electron of spin s in an orbital Y_{1m}. By setting $\mu \to \epsilon$ we can discard the second term.

The H_g vibration field is

$$u(\hat{\Omega}) = \frac{1}{\sqrt{2}} (Y^*_{2M}(\hat{\Omega}) b^\dagger_{MI} + Y_{2M}(\hat{\Omega}) b_{MI}) \ , \tag{3}$$

where $\hat{\Omega}$ is a unit vector on the sphere. The t_{1u} electron field is

$$\psi_s(\hat{\Omega}) = \sum_{m=-1}^{1} Y_{1m}(\hat{\Omega}) c_{ms} \ . \tag{4}$$

The electron–vibron interaction is local and rotationally invariant. Its form is completely determined (up to an overall coupling constant g) by symmetry:

$$H^{e-v} \propto g \int d\hat{\Omega} u(\hat{\Omega}) \sum_s \psi^\dagger_s(\hat{\Omega}) \psi_s(\hat{\Omega}) \ . \tag{5}$$

Using the relation

$$\int d\hat{\Omega} \ Y_{LM}(\hat{\Omega}) Y_{lm_1}(\hat{\Omega}) Y_{lm_2}(\hat{\Omega}) \propto (-1)^M \langle L, -M | lm_1; lm_2 \rangle \ , \tag{6}$$

where $\langle \cdots \rangle$ is a Clebsch-Gordan coefficient [16], yields the second quantized Hamiltonian

$$\begin{aligned} H^{e-v} \ = \ & \frac{\sqrt{3}}{2} g\hbar\omega \sum_{s,M,m} (-1)^m \left(b^\dagger_{MI} + (-1)^M b_{-MI} \right) \\ & \times \langle 2, M | 1, -m; 1, M+m \rangle c^\dagger_{ms} c_{M+ms} \ . \end{aligned} \tag{7}$$

The coupling constant g is fixed by the convention of O'Brien, who studied first this kind of dynamical JT problem [17]. Representation (7) is convenient for setting up an exact diagonalization program in the truncated Fock space.

2.1 The Real Representation

The semiclassical expansion is simpler to derive in the real coordinates representation. The vibron coordinates are

$$q_\mu = \frac{6}{\sqrt{10}} \sum_{m=-2}^{2} M_{\mu m} \left(b_m^\dagger + (-1)^m b_{-m} \right) , \tag{8}$$

where

$$\begin{aligned} M_{\mu,m\neq 0} &= (2 \text{ sign}(\mu))^{-\frac{1}{2}} \left(\delta_{\mu,m} + \text{sign}(\mu) \delta_{\mu,-m} \right) , \\ M_{\mu,0} &= \delta_{\mu,0} . \end{aligned} \tag{9}$$

$\{q_\mu\}$ are coefficients of the real spherical functions

$$\begin{aligned} f_\mu(\hat{\Omega}) &= \frac{6}{\sqrt{5}} \sum_m M_{\mu,m} Y_{2m}(\hat{\Omega}) \\ &= \begin{cases} \frac{6}{\sqrt{10}} \, Re \left(Y_{2|\mu|}(\hat{\Omega}) \right) & \mu = 1,2 \\ \frac{6}{\sqrt{5}} \, Y_{20}(\hat{\Omega}) & \mu = 0 \\ \frac{6}{\sqrt{10}} \, Im \left(Y_{2|\mu|}(\hat{\Omega}) \right) & \mu = -1,-2 \end{cases} . \end{aligned} \tag{10}$$

We also choose a real representation for the electrons

$$\begin{aligned} c_{xs}^\dagger &= \frac{1}{\sqrt{2}} \left(c_{1s}^\dagger + c_{-1s}^\dagger \right) \\ c_{ys}^\dagger &= \frac{1}{i\sqrt{2}} \left(c_{1s}^\dagger - c_{-1s}^\dagger \right) \\ c_{zs}^\dagger &= c_{0s}^\dagger . \end{aligned} \tag{11}$$

Thus the Hamiltonian in the real representation is given by

$$\begin{aligned} H &= H^0 + H^{e-v} \\ H^0 &= \frac{\hbar\omega}{2} \sum_\mu \left(-\partial_\mu^2 + q_\mu^2 \right) \\ H^{e-v} &= g \frac{\hbar\omega}{2} \sum_s (c_{xs}^\dagger, c_{ys}^\dagger, c_{zs}^\dagger) \begin{pmatrix} q_0 + \sqrt{3} q_2 & -\sqrt{3} q_{-2} & \sqrt{3} q_1 \\ -\sqrt{3} q_{-2} & q_0 - \sqrt{3} q_2 & -\sqrt{3} q_{-1} \\ -\sqrt{3} q_1 & \sqrt{3} q_{-1} & -2 q_0 \end{pmatrix} \begin{pmatrix} c_{xs} \\ c_{ys} \\ c_{zs} \end{pmatrix} \end{aligned} \tag{12}$$

This form of the JT hamiltonian is well known [17, 2]. Since the Hamiltonian is rotationally invariant, its eigenvalues are invariant under simultaneous O(3) rotations of the electronic and vibronic representations.

3 Jahn–Teller Distortions (Classical)

In the classical limit, one can ignore the vibron derivative terms in (12), and treat $\vec{q} = \{q_\mu\}$ as frozen coordinates in H^{e-v}. The coupling matrix in H^{e-v} is diagonalized by [18]:

$$T^{-1}(\varpi) \begin{pmatrix} z - \sqrt{3}r & 0 & 0 \\ 0 & z + \sqrt{3}r & 0 \\ 0 & 0 & -2z \end{pmatrix} T(\varpi) \ , \tag{13}$$

where

$$T = \begin{pmatrix} \cos\psi & \sin\psi & 0 \\ -\sin\psi & \cos\psi & 0 \\ 0 & 0 & 1 \end{pmatrix} \begin{pmatrix} \cos\theta & 0 & \sin\theta \\ 0 & 1 & 0 \\ \sin\theta & 0 & \cos\theta \end{pmatrix} \begin{pmatrix} \cos\phi & \sin\phi & 0 \\ -\sin\phi & \cos\phi & 0 \\ 0 & 0 & 1 \end{pmatrix} . \tag{14}$$

$\varpi = (\phi, \theta, \psi)$ are the three Euler angles of the O(3) rotation matrix T. In the diagonal basis of (13), the electron energies depend only on two vibron coordinates:

$$\vec{q}(0) = \begin{pmatrix} r \\ 0 \\ z \\ 0 \\ 0 \end{pmatrix} . \tag{15}$$

By rotating the vibron coordinates $\vec{q}$ to the diagonal basis using the $L = 2$ rotation matrix $D^{(2)}$ [16], one obtains

$$\vec{q}_\mu(r, z, \varpi) = \sum_{m,m',\mu'=-2}^{2} M_{\mu,m} D^{(2)}_{m,m'}(\varpi) M^{-1}_{m'\mu'} \vec{q}_{\mu'}(0) \ , \tag{16}$$

where $M_{\mu,m}$ was defined in (9).

By (16), and the unitarity of D and M, $|\vec{q}|^2$ is invariant under rotations of ϖ. Thus, the adiabatic potential energy V depends only on r, z, and the occupation numbers of the electronic eigenstates n_i, where $\sum_i n_i = n$.

$$V(z,r,[n_i]) = \frac{\hbar\omega}{2}(z^2+r^2) \; + \frac{\hbar\omega g}{2}\left(n_1(z-\sqrt{3}r) + n_2(z+\sqrt{3}r) - n_3 2z\right). \tag{17}$$

V is minimized at the JT distortions $(\bar{z}_n, \bar{r}_n, \bar{n}_i)$, at which the classical energy is given by

$$E_n^{cl} \; = \min \, V(\bar{z}_n, \bar{r}_n, \bar{n}_i). \tag{18}$$

The JT distortions at different fillings are given in Table I. We define $\tilde{\phi}, \tilde{\theta}$ as the longitude and latitude with respect to the diagonal frame ("principal axes") labelled $(1,2,3)$ (3 is at the north pole). $\bar{z}, \bar{r}$ parametrize the Jahn-Teller distortion in the real representation (10), as

$$\langle u^{JT}(\tilde{\theta},\tilde{\phi})\rangle \; = \frac{\bar{z}}{2}(3\cos^2\tilde{\theta} - 1) \; + \frac{\bar{r}\sqrt{3}}{2}\sin^2\tilde{\theta}\cos(2\tilde{\phi}). \tag{19}$$

In Table I we present the values of the ground state JT distortions at all electron fillings. We see that electron fillings $n = 1, 2, 4, 5$ have *unimodal distortions* which are symmetric about the 3 axis, while $n = 3$ has a *bimodal*, about the 3 and 1 axes. The two types of distortions are portrayed in Fig. 1. we depict the distortions of (19) for the unimodal and bimodal cases.

4 Semiclassical Quantization

At finite coupling constant g, quantum fluctuations about the frozen JT distortion must be included. In order to carry out the semiclassical quantization, we define a natural set of five dimensional coordinates r, z, ϖ. ϖ parametrize the motion in the JT manifold (the valley in the "mexican hat" potential V) and r, z are transverse to the JT manifold, since V depends on them explicitly. The transformation $\vec{q}(r,z,\varpi)$ was given in (16), and was

derived explicitly in Ref. [18] to be

$$\begin{aligned}
q_2 &= z\frac{1}{2}\sqrt{3}\sin^2\theta\cos 2\phi + r\frac{1}{2}(1+\cos^2\theta)\cos 2\phi\cos 2\psi \\
&\quad -r\cos\theta\sin 2\phi\sin 2\psi \\
q_1 &= z\frac{1}{2}\sqrt{3}\sin 2\theta\cos\phi - r\frac{1}{2}\sin 2\theta\cos\phi\cos 2\psi \\
&\quad +r\sin\theta\sin\phi\sin 2\psi \\
q_0 &= z\frac{1}{2}(3\cos^2\theta - 1) + \bar{r}\frac{1}{2}\sqrt{3}\sin^2\theta\cos 2\psi \\
q_{-1} &= z\frac{1}{2}\sqrt{3}\sin 2\theta\sin\phi - r\frac{1}{2}\sin 2\theta\sin\phi\cos 2\psi \\
&\quad -r\sin\theta\cos\phi\sin 2\psi \\
q_{-2} &= z\frac{1}{2}\sqrt{3}\sin^2\theta\sin 2\phi + r\frac{1}{2}(1+\cos^2\theta)\sin 2\phi\cos 2\psi \\
&\quad -r\cos\theta\cos 2\phi\sin 2\psi \ . \qquad (20)
\end{aligned}$$

The velocity in R^5 is given by

$$\dot{\vec{q}}(r(t), z(t), \varpi(t)) = \partial_r\vec{q}\dot{r} + \partial_z\vec{q}\dot{z} + \partial_\varpi\vec{q}\cdot\dot{\varpi} \ . \qquad (21)$$

Using (20) and (21), we calculate the classical kinetic energy in terms of the JT coordinates. After some cumbersome, but straightforward, algebra the kinetic energy is obtained in the compact and instructive form:

$$\begin{aligned}
\frac{1}{2}|\dot{\vec{q}}|^2 &= \frac{1}{2}\left(\dot{z}^2 + \dot{r}^2 + \sum_{i=1}^{3} I_i\omega_i^2\right), \\
\omega_1 &= -\sin\psi\dot{\theta} + \cos\psi\sin\theta\dot{\phi}, \\
\omega_2 &= \cos\psi\dot{\theta} + \sin\psi\sin\theta\dot{\phi}, \\
\omega_3 &= \dot{\psi} + \cos\theta\dot{\phi} \\
(I_1, I_2, I_3) &= \left((\sqrt{3}z + r)^2, (\sqrt{3}z - r)^2, 4r^2\right) . \qquad (22)
\end{aligned}$$

For finite JT distortions, we can identify the Euler angles terms as the kinetic energy of a rigid body rotator [19], and the quantities $I_i(\bar{z}, \bar{r})$ as moments of

inertia in the principle axes frame 1,2,3. Thus, the Euler angles dynamics follows that of a *rigid body rotator* [16].

The unimodal and bimodal cases will be discussed separately.

4.1 Unimodal Distortions

For the unimodal cases (which we found for the ground states of $n = 1, 2, 4, 5$, $\bar{r} = 0$ on the JT manifold. The "moments of inertia" in (22) are given by the tensor

$$\hat{I} = 3\bar{z}^2 \begin{pmatrix} 1 & 0 & 0 \\ 0 & 1 & 0 \\ 0 & 0 & 0 \end{pmatrix} . \tag{23}$$

This corresponds to the rotational energy of a point particle on a sphere, which is described by the angles θ, ϕ, and moment of inertia $3\bar{z}^2$. Since axis 3 has no "mass", its angular velocity is dominated by $\dot{\psi}$. This implies that we must keep the term $r^2\dot{\psi}^2$ but can discard the smaller mixed terms $\dot{\psi}\dot{\phi}$. This yields

$$\frac{1}{2}|\dot{\vec{q}}|^2 \approx \frac{1}{2}\left(\dot{z}^2 + \dot{r}^2 + r^2(2\dot{\psi})^2 \ + 3\bar{z}^2\left(\dot{\theta}^2 + \sin^2\theta\dot{\phi}^2\right)\right) . \tag{24}$$

The angular velocity $\dot{\psi}$ couples to r^2 as in the kinetic energy of a three dimensional vector $\mathbf{r}$ parameterized by the cylindrical coordinates

$$\mathbf{r} \ = (r\cos(2\psi), r\sin(2\psi), z - \bar{z}). \tag{25}$$

For $|\mathbf{r}| << \bar{z}$, the potential is simply

$$V(\mathbf{r}) \ \approx \frac{1}{2}|\mathbf{r}|^2 . \tag{26}$$

Thus, the semiclassical Hamiltonian of the unimodal distortion is

$$\begin{aligned} H^{uni} \ &\approx \ H^{rot} + H^{ho} \\ H^{rot} \ &= \ \frac{\hbar\omega}{6\bar{z}^2}\vec{L}^2 \\ H^{ho} \ &= \ \hbar\omega\sum_{\gamma=1}^{3}(a_\gamma^\dagger a_\gamma + \frac{1}{2}) \ , \end{aligned} \tag{27}$$

where $\vec{L}$ is an angular momentum operator, and H^{ho} are the three harmonic oscillator modes of r. The energies are given by

$$E^{uni} = \hbar\omega \left(\frac{1}{6\bar{z}_n^2} L(L+1) + \sum_{\gamma=1}^{3} (n_\gamma + \frac{1}{2}) \right) . \tag{28}$$

The rotational part of the eigenfunctions is

$$\Psi^{rot}_{Lm}(\vec{q}) = Y_{Lm}(\hat{\Omega}) \; |[n_{is}]\rangle_{\hat{\Omega}} \; , \tag{29}$$

where $\hat{\Omega} = (\theta, \phi)$ is a unit vector, and $|[n_{is}]\rangle_{\hat{\Omega}}$ is the electronic adiabatic ground state. It is a Fock state in the *principal axes* basis. In terms of the stationary Fock basis $|[n_{\alpha s'}]\rangle$ where $\alpha = x, y, z$, the adiabatic ground state is

$$|[n_{is}]\rangle_{\hat{\Omega}} = \sum_{[n_{\alpha s}]} \langle [n_{\alpha s}] | [n_{is}] \rangle_{\hat{\Omega}} |[n_{\alpha s}]\rangle. \tag{30}$$

Each overlap is a Slater determinant which is a sum of n products of spherical harmonics

$$\langle [n_{\alpha s}] | [n_{is}] \rangle_{\hat{\Omega}} = \sum_{[\nu]} C_{[\nu]} Y_{1\nu_1}(\hat{\Omega}) Y_{1\nu_2}(\hat{\Omega}) \cdots Y_{1\nu_n}(\hat{\Omega}) \; , \tag{31}$$

where $C_{[\nu]}$ are constants.

Now we discuss how boundary conditions determine the allowed values of L. A reflection on the JT manifold is given by

$$\hat{\Omega} \; \rightarrow -\hat{\Omega}. \tag{32}$$

Spherical harmonics are known to transform under reflection as

$$Y_{Lm} \rightarrow (-1)^L Y_{Lm} \; . \tag{33}$$

Thus, by (30) and (31), the electronic part of the wave function transforms as

$$|[n_{is}]\rangle_{\hat{\Omega}} \rightarrow (-1)^n |[n_{is}]\rangle_{-\hat{\Omega}} \; . \tag{34}$$

The reflection (32) can be performed by moving on a *continuous path* on the sphere from any point to its opposite. (See Fig. 2). It is easy to verify, using (16) or (20), that this path *is a closed orbit of* $\vec{q} \in R^5$:

$$\vec{q}(\hat{\Omega}) \rightarrow \vec{q}(-\hat{\Omega}) = \vec{q}(\hat{\Omega}) \ . \tag{35}$$

Thus we find that the electronic wave function yields a *Berry phase factor* of $(-1)^n$ for rotations between opposite points on the sphere which correspond to closed orbits of $\vec{q}$. In order to satisfy (29)) using the invariance of the left hand side under reflection, the pseudorotational Y_{Lm} wavefunction must cancel the electronic Berry phase. This amounts to a *selection rule* on L:

$$(-1)^{L+n} = 1 \ . \tag{36}$$

Thus, the ground state for $n = 1$ and 5 electrons has pseudo-angular momentum $L = 1$ and finite zero point energy due to the non trivial Berry phases.

4.2 Bimodal Distortion

The analysis of the bimodal distortions $n = 3$ proceeds along similar lines. The distortion obeys

$$\bar{z} = \sqrt{3}\bar{r} \ . \tag{37}$$

From Eq.(22) we see that the kinetic energy is given by

$$\frac{1}{2}|\dot{\vec{q}}|^2 = \frac{1}{2}\left(\dot{z}^2 + \dot{r}^2 + \sum_{i=1}^{3} I_i \omega_i^2\right) , \tag{38}$$

where the inertia tensor is

$$\hat{I} = 2\bar{z}^2 \begin{pmatrix} 4 & 0 & 0 \\ 0 & 1 & 0 \\ 0 & 0 & 1 \end{pmatrix} . \tag{39}$$

The quantization of the pseudo–rotational part is the quantum symmetric top Hamiltonian. Fortunately, it is a well-known textbook problem (see e.g.

Ref. [20, 16]). The eigenfunctions of a rigid body rotator are the rotational matrices

$$D^{(L)}_{mk}(\varpi), \tag{40}$$

where L, m, k are quantum numbers of the commuting operators $\vec{L}^2, L^z, L^1$ respectively. L^z and L^1 are defined with respect to the fixed z axis and the co-rotating 1 axis respectively. The quantum numbers are in the ranges

$$\begin{aligned} L &= 0, 1, \ldots \infty \\ m, k &= -L, -L+1, \ldots L \ . \end{aligned} \tag{41}$$

The remaining coordinates are two massive harmonic oscillators modes

$$\mathbf{r} = (r - \bar{r}, z - \bar{z}). \tag{42}$$

The semiclassical Hamiltonian is thus

$$\begin{aligned} H^{bi} &\approx H^{rot} + H^{ho}, \\ H^{rot} &= \frac{\hbar\omega}{4\bar{z}^2}\vec{L}^2 - \frac{3\hbar\omega}{16\bar{z}^2}(L^1)^2, \\ H^{ho} &= \hbar\omega \sum_{\gamma=1}^{2}(a^\dagger_\gamma a_\gamma + \frac{1}{2}), \end{aligned} \tag{43}$$

and its eigenvalues are

$$E^{bi} = \hbar\omega \left(\frac{1}{4\bar{z}^2}L(L+1) - \frac{3}{16\bar{z}^2}k^2 \ + \sum_{\gamma=1}^{2}(n_\gamma + \frac{1}{2}) \right). \tag{44}$$

The rotational eigenfunctions are explicitly dependent on ϖ as

$$\Psi^{rot}_{Lmk}[\vec{q}] = D^{(L)}_{mk}(\varpi) \prod_{is} |n_{is}\rangle_\varpi \ . \tag{45}$$

4.3 Berry Phases of a Bimodal Distortion

Unlike the unimodal case, in the bimodal case no single reflection fully classifies the symmetry of the wavefunction. However, one can obtain definite

sign factors by transporting the electronic ground state in certain orbits. We define the rotations of π about principle axis L^i as C_i, which are schematically depicted in Fig. 3. The Berry phases associated with these rotations can be read directly from the rotation matrix T in Eq. (14). For example: for $\psi \rightarrow \psi + \pi$ (C_3), the states $|1\rangle$ and $|2\rangle$ get multiplied by (-1).

Since $D^{(L)}_{m,k}$ transform as Y_{Lk} under C_i, it is easy to determine the sign factors of the pseudorotational wavefunction. The results are given below:

$$\begin{aligned} C_1 &: |1,0,2\rangle_{\varpi} \rightarrow |1,0,2\rangle_{\varpi'} \qquad & C_1 &: D^{(L)}_{m,k} \rightarrow (-1)^k D^{(L)}_{m,k} \\ C_2 &: |1,0,2\rangle_{\varpi} \rightarrow -|1,0,2\rangle_{\varpi'} \qquad & C_2 &: D^{(L)}_{m,k} \rightarrow (-1)^{L+k} D^{(L)}_{m,-k} \\ C_3 &: |1,0,2\rangle_{\varpi} \rightarrow -|1,0,2\rangle_{\varpi'} \qquad & C_3 &: D^{(L)}_{m,k} \rightarrow (-1)^{L} D^{(L)}_{m,-k} \ . \end{aligned} \tag{46}$$

$\vec{q}$ are coefficients in an $L = 2$ representation, and therefore are invariant under C_1, C_2, C_3. C_i describe continuous closed orbits in R^5. In order to satisfy (46) and using the degeneracy of E^{bi} for $k \rightarrow -k$, we find that

$$L = \text{odd} \ , \qquad k = \text{even}. \tag{47}$$

In particular, the ground state of (45) is given by $L=1$, and $k=0$.

4.4 High-Spin Polarized Ground States

It is possible to repeat the semiclassical analysis assuming that the spins are maximally polarized. These high-spin states are important, as they tend to prevail for strongly repulsive intra-level Hubbard U (Hund's rule) situations. In this case, we determine the JT distortions considering the Pauli exclusion between likewise spins. In Table II the JT distortions of the spin polarized ground states are listed. Our results for n=2,4 (S=1), and n=3 (S=3/2) cases are presented. The latter is trivial, since in that case $n_1 = n_2 = n_3 = 1$, and therefore there is no JT effect at all. For n=2, (S=1) there is unimodal distortion of $\bar{z} = -g$ which is smaller than the unpolarized ground state, and is equal to the distortion of the $n = 5$ case. Inspection of the orbital

energies $\epsilon_1 = \epsilon_2 = -g$, $\epsilon_3 = 2g$ provides a clear explanation for the identical distortions of the n=2 (S=1) and n=5 ($S = \frac{1}{2}$) cases, since in both cases ϵ_3 is occupied by a "spin up hole".

Electronically, however, the two states are very different. First, we do not have a Berry phase for even number of electrons, as the individual contributions from each of the two electrons cancel out. Second, there is a nonzero *electronic* orbital angular momentum. For example, the symmetry of the two-electron state prior to JT distortion is ^{3}P (i.e. $^3t_{1u}$), and so it remains following dynamical JT [21]. At finite coupling the two electrons in their ground state are still coupled in a ^{3}P electronic state, with L_{orb}=1, where L_{orb} is the electronic orbital angular momentum, not to be confused with the pseudorotational quantum number L. Due to the absence of a Berry phase L must in fact be even, in contrast with the single electron case, and in agreement with Eq. (36). Thus although both cases have threefold degeneracies, they arise from different physical motion: purely electronic (for the n=2, S=1 case) versus mixed electron–vibron motion (in the n=5, S=1/2 case).

5 Exact Diagonalization

The above semiclassical scheme gives a clear and intuitive picture of the behaviour of the system in a strong coupling limit. This limit is appropriate for describing, e.g., Na_3 [10]. However, in C_{60} the actual range of the coupling parameter - $g \approx 0.3$ for a typical mode [22, 15] - suggests that the electron–vibron coupling is actually in the weak to intermediate regime.

Here we diagonalize the electron–vibron Hamiltonian (7) for single H_g mode in a truncated Fock space. This approach yields accurate results unless the coupling strength is too large, and the higher excited vibrons admix strongly into the low lying states. We compare the results to the asymptotic large g expressions of the semiclassical approximation. The ground state energy for $n = 1$ has been previously computed in this fashion by O'Brien

[18]. Here we present detailed results for all electron occupations, and also for the excitation spectra.

Our basis is the finite dimensional Fock space of electrons and vibrons,

$$\left\{ |n_{Mf}, n_{ms}\rangle \quad : \quad N_v \leq N^{max}, \sum_{ms} n_{ms} = n \right\}, \tag{48}$$

where $N_v = \sum_{Mf} n_{Mf}$ is the total vibron occupation. By gradually increasing N^{max}, we have found empirically that accurate results can be obtained for $g \leq N^{max}/2$, for levels with unperturbed energy below $\hbar\omega N^{max}/2$. In particular, we have chosen $N^{max} = 5$ (for $n = 2, 3$) which yields an accuracy of better than $0.05\hbar\omega$ for $g \leq 0.6$ and levels with $N_v \leq 1$. The effect of truncation is a general upward shift of the levels, which gradually increases for higher excited levels. Level splittings and excitation energies are therefore less sensitive to the cutoff error.

In Figures 4, 5 and 6 the ground state and a few of the excited states energies are plotted for one two and three electrons respectively. The four and five electron spectra are related to the two and one electron spectra by particle–hole symmetry. Energies are plotted as functions of g^2. We compare the results to the semiclassical expressions (28) and (44) for large coupling, and to second order perturbation theory at weak coupling. We discuss the different cases in detail, below.

5.1 $n = 1, 5$ electrons

The ground state for one electron or hole in the t_{1u} shell is a threefold-degenerate state (all degeneracies given do not include spin) of the same symmetry: this fact is in complete analogy with what happens in the $e \otimes E$ coupled system, where the final dynamical JT coupled ground state has again E symmetry [21]. Additional splitting of this ground state could occur via spin-orbit coupling, not included in the present treatment. Recent spectroscopic data [23] of C_{60}^- embedded in solid Ar confirm indirectly the presence

of the pseudorotational $L = 1$ ground state degeneracy, through direct observation of spin-orbit splittings of about 30 and of 75 cm^{-1} for the t_{1u} ground state and for the t_{1g} excited electronic state $\approx$ 1 eV above. The decrease of ground state energy is initially fast, and becomes gradually slower for increasing g. We shall return to this point in detail in [15].

As shown in Fig. 4, for large g, the n=1 ground state energy correctly approaches the strong coupling limit

$$E \sim -\frac{1}{2}g^2 + \frac{3}{2} + \frac{1}{3g^2} , \tag{49}$$

except for a small shift due, as mentioned above, to a finite-cutoff error. Above the ground state, there are families of excitations, corresponding to increasing values of N_v. The lowest, for $N_v = 1$, comprises $3 \times 5 = 15$ states, since for n=1, N_v=1 there are just 3 electron states and 5 vibron states available. These states correspond to a direct product of a P (electronic) and a D (vibrational) manifold. As elementary angular momentum theory requires, they split into $L = 3$, 2 and 1 levels, which are found, in order of increasing energy. The splitting initially is proportional in g^2, for small g, with significant deviations from linearity at $g^2 \approx 0.2$. As coupling increases, we note the slower downward trend of the *even* L states, than both the ground state and the associated "soft" odd-L excitations. This clearly reflects the Berry phase selection rule (36) that *no even L should appear among the low lying excited states* in strong coupling. The lowest excitation from the ground state is L=1$\rightarrow$ L=3, anticipating already at very weak coupling the strong coupling result that this excitation energy should fall fastest, and collapse as $\frac{5}{3g^2}$. Unlike the L=3 state, the L=2 and L=1 excited states do not show any tendency to collapse onto the ground state in the large g limit. Therefore they can be seen as modes involving essentially radial massive vibrations.

The next group of excitations is for $N_v = 2$, and comprise $3 \times 15 = 45$ states. This multiplet splits into seven levels corresponding to $L = 5$, 3, 1, 4, 2, 1 and 7. The lowest (L=5) level crosses two levels of the lower

(N_v=1) multiplet in its downwards motion to become the second excited state above the L=3 level, eventually constituting the low energy odd-L rotational multiplet of the strong coupling picture. The same route is followed by the lowest level of $N_v = 3$, which is an L=7 state. In fact, all the lowest split levels from each N_v multiplet appear to have L=$2N_v + 1$ and follow the same route.

For $N_v = 2$ we can similarly follow the movement with g of the L=4 level which decreases slowly towards the L=2 state from the lower $N_v = 1$ to add to the group of massive radial vibrations.

5.2 $n = 2, 4$ electrons

Figure 5 has several features which contrast sharply with the one electron case. The $N_v = 0$ multiplet, has 15 two-electron states. The spin singlet subspace constitutes of a 6-fold degenerate multiplet that splits into an orbital S and a D multiplet. As the semiclassical Eq. (36) suggests, the ground state and lowest excitations in the strong coupling limit have orbital degeneracies of *even* angular momenta. In fact, the lowest two among these states (L = 0, 2) both come from the N_v=0 multiplet, in contrast with the one electron case. The next pseudorotational level ($L = 4$) originates in the $6 \times 5 = 30$-fold degenerate $N_v = 1$, spin singlet multiplet. Actually, at weak coupling it starts out being second in the ordering (L= 2, 4, 3, 2, 1, 0), but already at very small g it crosses the lower L=2 partner and approaches the pseudo–rotational asymptotic level. The convergence with increasing cutoff N^{max} is worse than in the n=1 case, which can be as due to larger JT distortions associated with two electrons. The spin triplet (S=1) states of n=2 have not been plotted, as they behave in exactly the same fashion as the n=1 states (see Fig. 4). This figure can be read in terms of n=2 S=1 states simply by replacing the spin multiplicity label 2, as was in the case n=1, with 3. By comparison of Fig. 5 and Fig. 4 we notice that the low-spin ^{1}P state of N_v=1

is exactly degenerate with the high-spin ^{3}D state in the same multiplet. This degeneracy seems accidental.

5.3 $n = 3$ electrons

For three electrons, the results are shown in Fig. 6. The 8-fold degenerate $N_v = 0$ multiplet splits into two states characterized by degeneracies 3 and 5 (^{2}P and ^{2}D). The ground state has the correct symmetry for an L=1, k=0 state, which is predicted to be the ground state in the semiclassical limit. We also expect the lowest excitations to be classified as L=3, k=2 (14-fold degenerate), and L=3, k=0 (7-fold degenerate). In fact, three levels from the $N_v = 1$ multiplet move down toward the ground state for increasing g. The one which moves lowest is 9-fold (^{2}G). In the $g \to \infty$ limit, it must therefore merge with the 5-fold levels from the N_v=0 multiplet to produce the expected L=3, k=2 pseudo–rotator excitation. The next excitation of L=3, k=0 state can be identified as an asymptotic limit of the ^{2}F 7-fold degenerate state seen in Fig. 6.

A remarkable feature of the $n = 3$ case is the presence in the $N_v = 1$ multiplet of a state (the ^{2}S) whose energy is independent of g! This state is degenerate with the S=3/2 state ^{4}D which has no JT distortion.

6 Pair Binding Energies

The *pair energy* for an average filling of n electrons is defined as

$$U_n = E_{n+1} + E_{n-1} - 2E_n \ , \tag{50}$$

where E_n are the fully relaxed ground state energies of n electrons. Formally, U is the real part of the two–electron vertex function at zero frequency. If this energy is negative for odd values of n, it means that electrons will have lower total energy if they separate into $(n-1)$ and $(n+1)$ occupations of

different molecules, rather than occupying n electrons on all molecules. For odd values of n, this is an effective pairing interaction often called "pair binding" in the literature [5]. In Section 4 we found that for all odd n, the pair energies are negative, and given by the large g asymptotic expression

$$U_{n=1,3,5} \sim -g^2 + 1 - \frac{2}{3g^2} + \mathcal{O}(g^{-4}). \tag{51}$$

The first term is the *classical energy.* The second term is due to reduction of zero point energy along the JT manifold, since only radial modes remain hard. This term is independent of g and positive. The last term is due to the quantum pseudo–rotator Hamiltonian, and the Berry phases which impose a finite ground state energy associated with odd L for odd numbers of electrons. This term, although nominally small at large g, becomes important at weaker coupling. If (51) is extrapolated to the weak coupling regime the last term would dominate the pair binding energy. The exact diagonalization shown in Figure 7, indeed shows a significant enhancement of the pair binding energy over the classical value in the weak coupling regime.

In the weak coupling limit, we can obtain analytical expressions for $U_n(g)$ for $g << 1$ by second order perturbation theory. The unperturbed Hamiltonian is the non interacting part H^0 with eigenstates (48). The perturbing hamiltonian is H^{e-v} of Eq. (7), which connects Fock states differing by one vibron occupation. All diagonal matrix elements vanish, and the leading order corrections to any degenerate multiplet are of order g^2. These are given by diagonalization of the matrix [24],

$$\Delta^{(2)}_{n_{ms},n'_{ms}} = \langle 0, n_{ms}|H^{e-v}\frac{1}{E_a^{(0)} - H^0}H^{e-v}|0, n'_{ms}\rangle, \tag{52}$$

in the degenerate 0-vibrons subspace. The sum implied by the inverse operator $(E_a^{(0)} - H^0)^{-1}$ extends just to the N_v=1 states. The eigenvalues of $\Delta^{(2)}$ yield the ground state energies and splittings for different electron fillings. These results, for all H_g and also A_g modes, and extended to the N_v=1 multiplet, will be discussed more extensively in [15].

Here we refer only to ground state energetics. In particular, using the perturbative expressions, we obtain, for a single H_g, mode the small g pair binding energy

$$\frac{U_{n=1,3,5}}{\hbar\omega} = -\frac{5}{2}g^2 + \mathcal{O}(g^4). \tag{53}$$

The dependence strictly on powers of g^2 alone, with absence of all odd powers, is a consequence of the already mentioned $\Delta N_v = \pm 1$ selection rule of Eq. (7). The origin of the 5/2 factor that characterizes the perturbative result (53) with respect to the classical pair binding energy (Table I) will be discussed in Ref. [15].

The molecular pair binding energy can be considered as an effective negative-U Hubbard interaction for the lattice problem, provided that the Fermi energy ϵ_F is not much larger than the JT frequency scale ω. A mean field estimate of the transition temperature for the negative-U Hubbard model in the weak coupling regime is [25, 5]

$$T_c \approx \epsilon_F \exp\left[(-N(\epsilon_F)|U|)^{-1}\right]. \tag{54}$$

In Refs. [3] and [26], the results of Migdal–Eliashberg approximation for the superconducting transition temperature was given. Without the Coulomb pseudopotentials this approach yields

$$\begin{aligned} T_c &\approx \omega \exp\left[(-N(\epsilon_F)|V|)^{-1}\right] \\ V &= -\frac{5}{6}g^2 . \end{aligned} \tag{55}$$

By comparing (53) to (55) we find a striking discrepancy between the values of the effective pairing interaction:

$$U = 3V. \tag{56}$$

That is to say: in the weak coupling regime, the correct molecular calculation yields a pairing interaction which is *three times larger* than the results of Migdal–Eliashberg theory.

7 Discussion

In this paper, we have solved the problem of a single H_g vibron coupled to t_{1u} electrons in a C_{60}^{n-} molecule. The model is too simplified for quantitative predictions for C_{60}, but it contains interesting novel physics which will be important for further studies of this system.

Semiclassically, a dynamical Jahn–Teller effect occurs. For $n = 1, 2, 4, 5$, the molecule distorts unimodally, giving rise to a pseudo-angular momentum spectrum, plus three harmonic oscillators. For $n = 3$, there is a bimodal distortion, which generates a spectrum of a symmetric top rotator, plus two harmonic oscillators. The pseudo rotations are subject to non trivial Berry phase effects, which determine the pseudo-angular momenta L, and thus the degeneracies and level ordering of the low lying states. Strong Berry phase effects seem to survive even at moderate and weak coupling as shown by the exact diagonalization results.

We find at weak coupling that the pair binding energy is a factor of 5/2 larger than the classical JT effect, and a factor of three larger than the pairing interaction of Migdal–Eliashberg theory of superconductivity. This enhancement can be interpreted semiclassically as due to large zero point energy reduction of the pseudo–rotations. From the weak coupling point of view, this effect is due to degeneracies in both electronic and vibronic systems.

Migdal's approximation neglects vertex corrections in the resummation of two–particle ladder diagrams. This is justified only in the retarded limit $\omega << \epsilon_F$. Here we have considered the opposite limit, where the molecular ground state energies are solved first, assuming that the JT relaxation time is of the same order, or faster than the inter molecular hopping time. In this regime, we have found therefore that Migdal's approximation substantially *underestimates* the pairing interaction, and T_c, for these ideal molecular solids [27]. This large effect suggests that some of the enhancement is likely to carry

over to the real case of A_3C_{60} metals, where electron hopping t and vibron frequencies are of similar strength.

In Part II we shall consider a more realistic model which includes all important vibron modes of C_{60}. We shall present quantitative predictions for the electron–vibron effects on the spectroscopy of C_{60} ions.

Acknowledgements

A.A. is indebted to Yossi Avron and Mary O'Brien for valuable discussions, and acknowledges the Sloan Foundation for a fellowship. ET and NM wish to acknowledge discussions with S. Doniach. This paper was supported by grants from the US-Israel Binational Science Foundation, the Fund for Promotion of Research at the Technion, and the US Department of Energy No. DE-FG02-91ER45441, the Italian Istituto Nazionale di Fisica della Materia INFM, the European US Army Research Office, and NATO through CRG 920828.

References

[1] A. F. Hebard, Phys. Today, Nov. 1992, p. 26, and references therein.

[2] C. M. Varma, J. Zaanen, and K. Raghavachari, Science, **254**, 989 (1991).

[3] M. Schlüter, M. Lannoo, M. Needels, G. A. Baraff, and D. Tománek, Phys. Rev. Lett.**68**, 526 (1991); J. Phys. Chem. Solids, **53**, 1473 (1992).

[4] R. A. Jishi, M. S. Dresselhaus, Phys. Rev. B **45**, 2597 (1992); M. G. Mitch, S. J. Chase, and J. S. Lannin, Phys. Rev. B **46** 3696 (1992).

[5] G. Baskaran and E. Tosatti, Current Science (Bangalore) **61**, 33 (1991); S. Chakravarty, M. Gelfand, and S. Kivelson, Science, **254**, 970 (1991); G. N. Murthy and A. Auerbach, Phys. Rev. B **46**, 331 (1992).

[6] K. H. Johnson, M. E. McHenry and D. P. Clougherty, Physica C **183**, 319 (1991).

[7] C. A. Mead, Rev. Mod. Phys., **64**, 51 (1992).

[8] *Geometric Phases In Physics*, edited by A. Shapere and F. Wilczek (World Scientific, Singapore, 1989).

[9] H. C. Longuet-Higgins, Adv. Spect. **2** 429, (1961), and references therein; G. Herzberg and H. C. Longuet-Higgins, Discuss. Faraday Soc. **35**, 77 (1963); H. C. Longuet-Higgins, Proc. Roy. Soc. London **A344**, 147 (1975); C. A. Mead and D. G. Truhlar, J. Chem. Phys., **70**, 2284 (1979).

[10] G. Delacrétaz, E. R. Grant, R. L. Whetten, L. Woste, and J. W. Zwanziger, Phys. Rev. Lett., **56**, 2598 (1986).

[11] B. Goss Levi, Phys. Today **46**, 17 (1993).

[12] E. Tosatti, Invited paper, Euroconference on Superconductivity, Pisa, Italy 21-25 Jan. 1993 (unpublished).

[13] J. Gonzalez, F. Guinea, and M. A. H. Vozmediano, Phys. Rev. Lett.**69**, 172 (1992).

[14] J. Ihm (1993) (unpublished).

[15] N. Manini, E. Tosatti, and A. Auerbach, Phys. Rev. B, subsequent paper.

[16] A. R. Edmonds, *Angular Momentum In Quantum Mechanics*, (Princeton University Press, Princeton, 1974).

[17] M. C. M. O'Brien, Phys. Rev. **187**, 407 (1969)

[18] M. C. M. O'Brien, J. Phys. C **4**, 2524 (1971).

[19] One should not confuse the pseudo–rotations of Eq. (22), which describe propagating vibrational waves, with real rotations of the molecule. In solid state those are assumed to be frozen out by crystal fields at the temperatures of interest. Moreover, for a real rigid body, each moment of inertia cannot exceed the sum of the other two [28].

[20] L. D. Landau and E. M. Lifshitz, *Quantum Mechanics* (Pergamon, Oxford, 1976), Ch. 13.

[21] F. S. Ham, Phys. Rev. Lett., **58**, 725 (1987).

[22] V. P. Antropov, A. Gunnarsson, and A. I. Liechtenstein, Phys. Rev. B **48**, 7651 (1993).

[23] Z. Gasyna, L. Andrews, and P. N. Schatz, J. Phys. Chem. **96**, 1525 (1991).

[24] J. J. Sakurai, *Modern Quantum Mechanics*, (Benjamin, Menlo Park, Calif., 1985).

[25] V. J. Emery, Phys. Rev. B. **14** 2989 (1976). A. Aharony and A. Auerbach, Phys. Rev. Lett., **70** 1874 (1993).

[26] M. Lannoo, G. A. Baraff, and M. Schluter, Phys. Rev. B 44, 12106 (1991).

[27] Our reason for the enhancement is different from those of other recent discussions of breakdown of Migdal-Eliashberg approximation, see e.g. L. Pietronero, Europhys. Lett. **17**, 365 (1992).

[28] L. D. Landau and E. M. Lifshitz, *Mechanics* (Pergamon, Oxford, 1960), Ch. 32.

Table I

n	S	$(\bar{z}_n, \bar{r}_n)$	$(\bar{n}_1, \bar{n}_2, \bar{n}_3)$	$E_n/(\hbar\omega)$	$U_n/(\hbar\omega)$
0	0	$(0,0)$	(0,0,0)	$\frac{5}{2}$	
1	$\frac{1}{2}$	$(g,0)$	(0,0,1)	$-\frac{1}{2}g^2+\frac{3}{2}+\frac{1}{3g^2}$	$-g^2+1-\frac{2}{3g^2}$
2	0	$(2g,0)$	(0,0,2)	$-2g^2+\frac{3}{2}$	
3	$\frac{1}{2}$	$(\frac{3}{2}g, \frac{\sqrt{3}}{2}g)$	(1,0,2)	$-\frac{3}{2}g^2+1+\frac{1}{3g^2}$	$-g^2+1-\frac{2}{3g^2}$
4	0	$(-2g,0)$	(2,2,0)	$-2g^2+\frac{3}{2}$	
5	$\frac{1}{2}$	$(-g,0)$	(2,2,1)	$-\frac{1}{2}g^2+\frac{3}{2}+\frac{1}{3g^2}$	$-g^2+1-\frac{2}{3g^2}$
6	0	$(0,0)$	(2,2,2)	$\frac{5}{2}$	

TABLE I. Semiclassical ground state distortions and energies for a single H_g coupled mode of frequency ω. n is the electron number, S is the total spin, $\bar{z}_n, \bar{r}_n$ are the JT distortions, $\bar{n}_i$ is the occupation of orbital i, E_n is the ground state energy and, and U_n is the pair energy (Eq.(50)). Energies are calculated for strong coupling to order g^{-2}.

Table II

n	S	$(\bar{z}_n, \bar{r}_n)$	$(\bar{n}_1, \bar{n}_2, \bar{n}_3)$	$E_n/(\hbar\omega)$
2	1	$(-g,0)$	(1,1,0)	$-\frac{1}{2}g^2+\frac{3}{2}$
3	$\frac{3}{2}$	$(0,0)$	(1,1,1)	$\frac{5}{2}$
4	1	$(g,0)$ (uni)	(1,1,2)	$-\frac{1}{2}g^2+\frac{3}{2}$

TABLE II. High spin ground state properties, in the same notation of Table I.

Figure 1: A polar representation of the Jahn-Teller distortions $u^{JT}(\tilde{\theta},\tilde{\phi})$, Eq.(19). The distortion is measured relative to a sphere. (a) The unimodal distortion for the ground states of $n = 1,2,4,5$ electrons (b) The bimodal distortion for $n = 3$ electrons.

Figure 2: Berry phase calculation for unimodal distortions. An path between reflected points on the unit sphere corresponds to a closed orbit in the five dimensional $\vec{q}$-space. According to Eq. (34), such a path acquires a Berry phase of $(-1)^n$ from the n-electron wavefunction.

Figure 3: Berry phases calculation for the bimodal distortion ($n = 3$). ϖ are the three Euler angles which rotate the principal axes of the bimodal distortion. C_i denote rotations by π around corresponding axes. On the right we depict the electronic Berry phases associated with the three closed orbits in $\vec{q}$-space, given by Eq. (46).

Figure 4: Exact spectrum for one electron as a function of the square electron–vibron coupling constant g^2. The vibron occupations are truncated at $N^{max} = 5$. The semiclassical energies (Eq. (28)) are drawn by dashed lines for the lowest three pseudorotational multiplets (n_γ=0, L=1, 3, 5). The unit of energy is the vibron quantum $\hbar\omega$.

Figure 5: Exact spectrum for two electrons ($S = 0$). The semiclassical energies (Eq. (28)) are drawn by dashed lines for the lowest three pseudorotational multiplets (n_γ=0, L=0, 2, 4). The two-electron $S = 1$ spectrum is the same as for $n = 1$, $S = \frac{1}{2}$.

Figure 6: Exact spectrum for three electrons ($S = \frac{1}{2}$). The semiclassical energies, Eq.(44), are drawn by dashed lines for the lowest three pseudorotational multiplets, n_γ=0, (L,k)=(1,0), (3,2) (3,0).

Figure 7: Pair binding energy U (thick solid line), compared to weak coupling perturbation theory for $g << 1$ (dotted line) and semiclassical theory for $g >> 1$ (dashed lines). U_n is found to be the same for $n = 1, 3, 5$ electrons. The Migdal–Eliashberg approximation V (thin solid line) is also drawn for comparison. $g^{C_{60}}$ is the range of physical coupling strength for C_{60}.

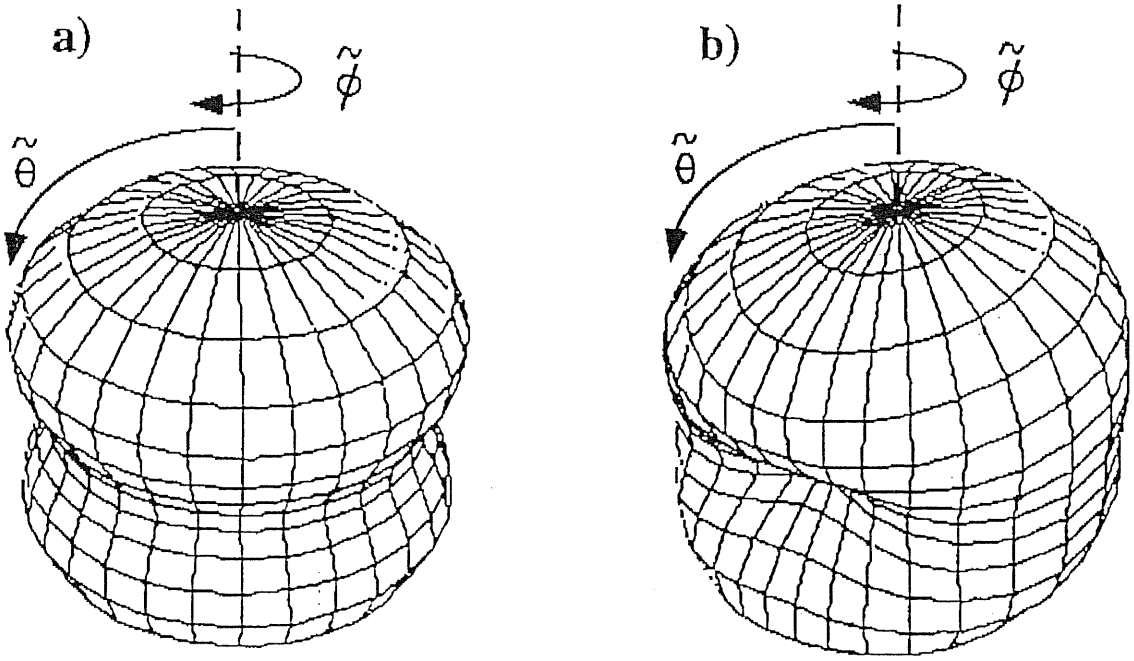

Auerbach, Manini, Balatsky (PART 1)

Fig 1

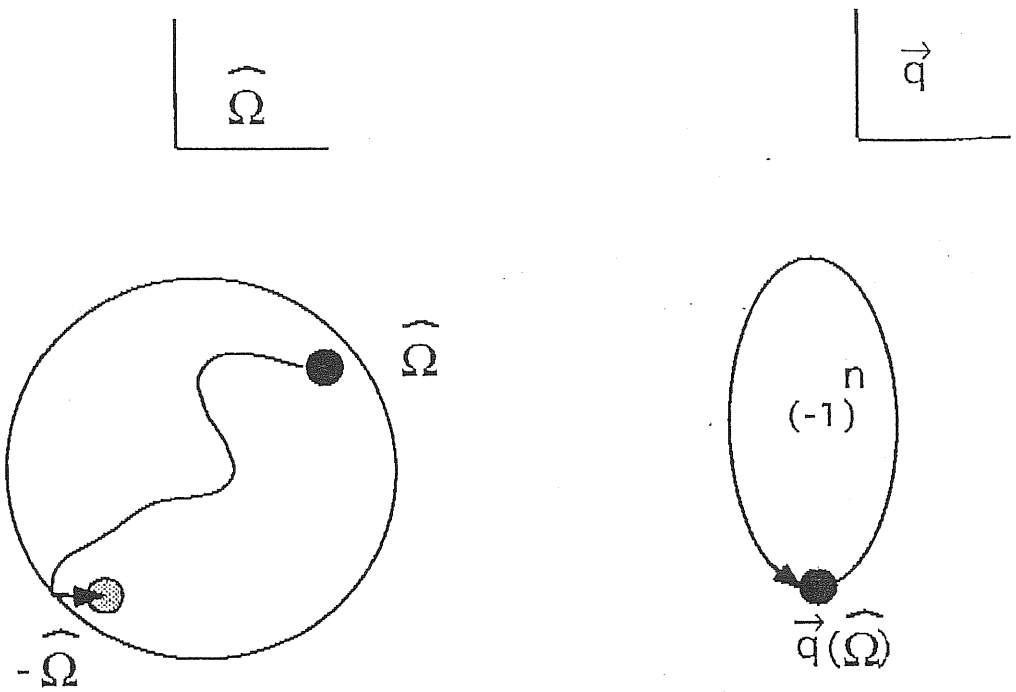

Auerbach, Manin, Read. (PART 1)

Fig. 2

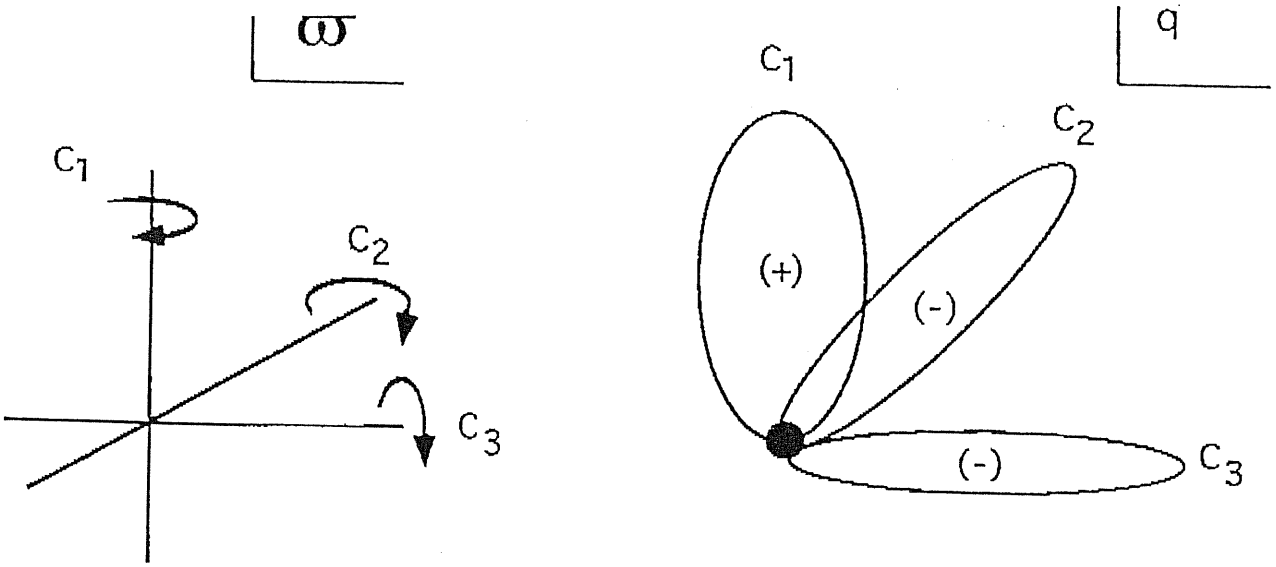

Auerbach, Manini, BSatt. (PART 1)

Fig. 3

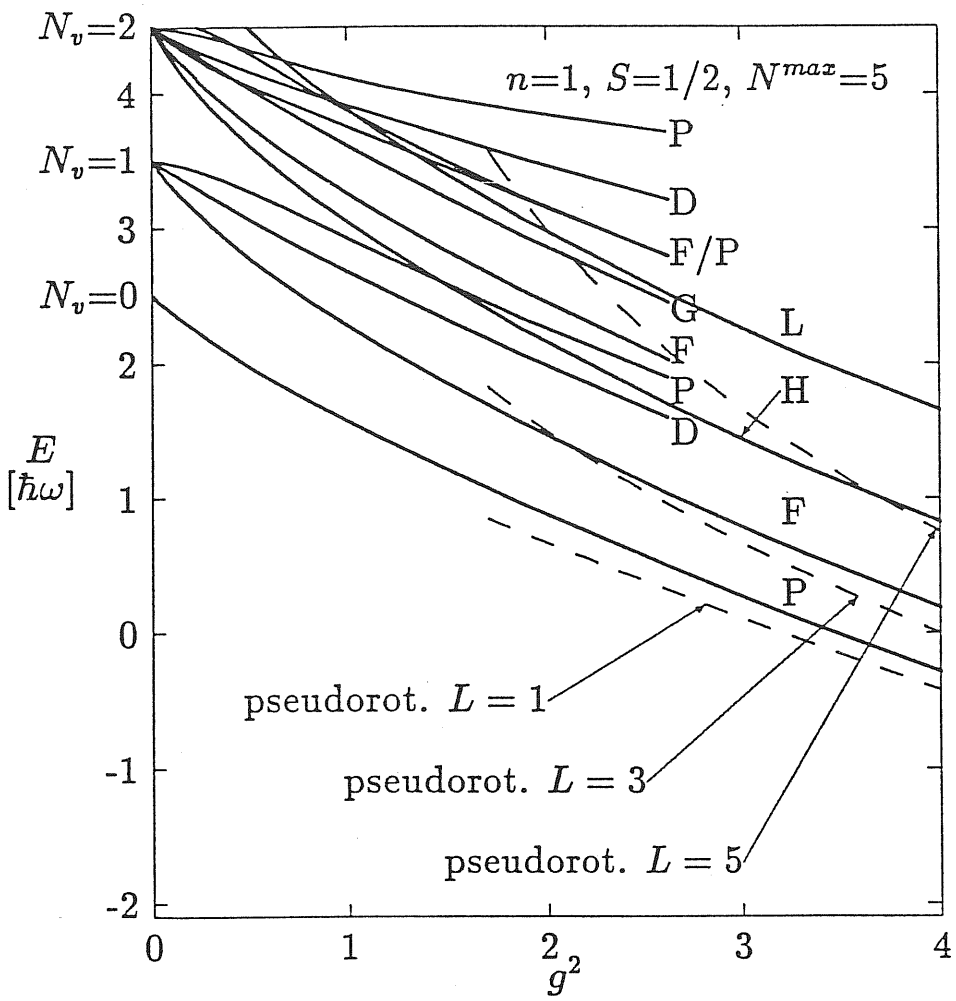

Auerbach Manini Trott. [Part I]

fig 4

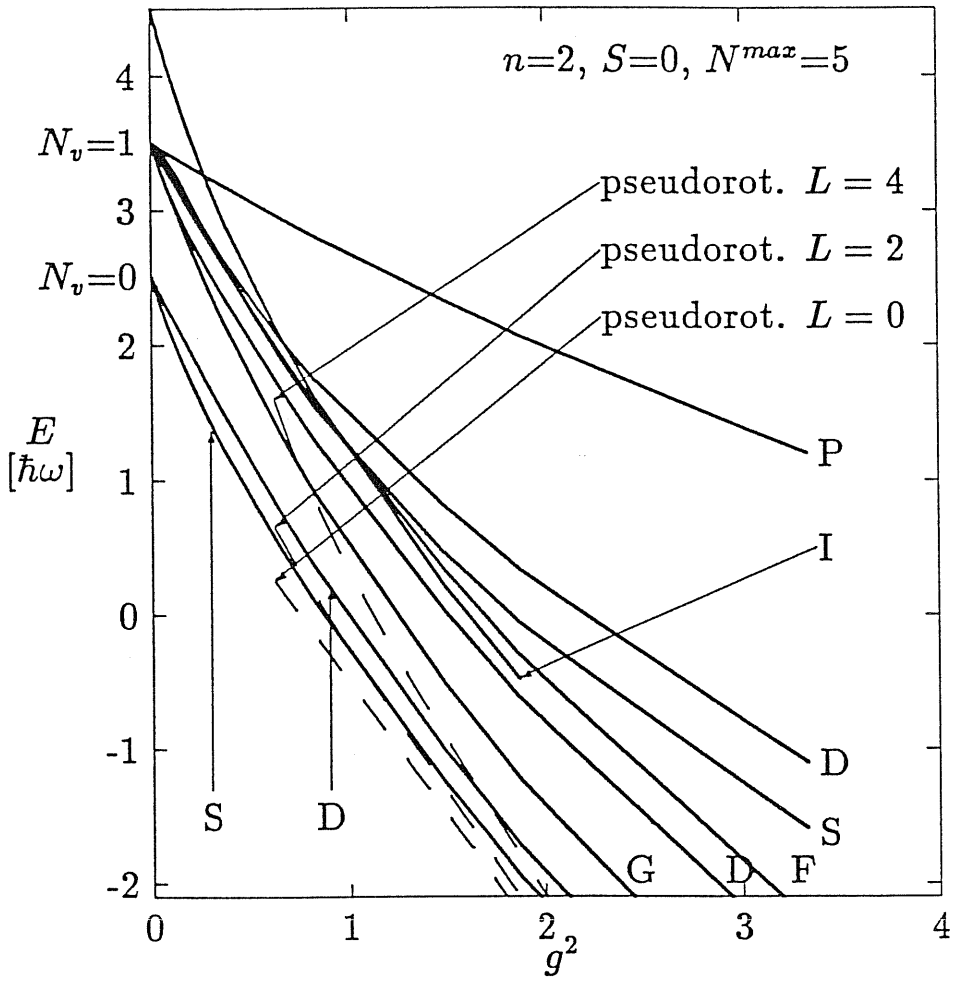

Auerbach Massini Tzabtti [Part I]

fig 5

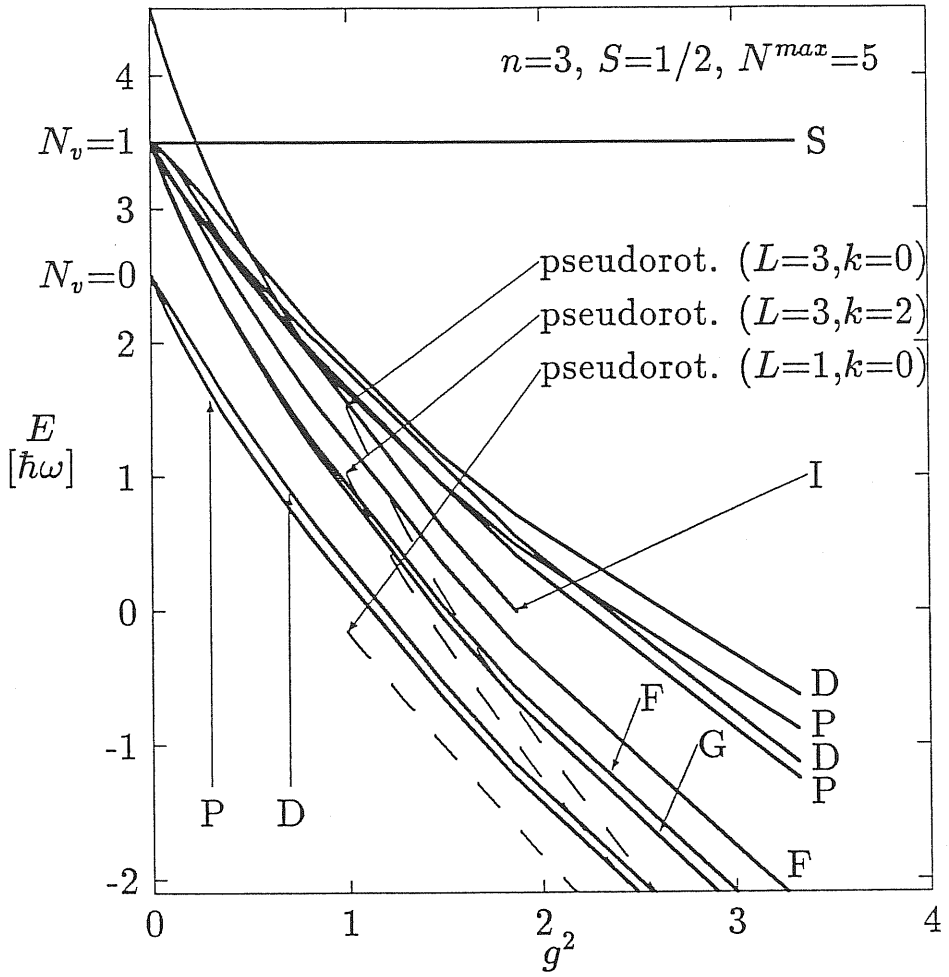

Auerbach Ramini Tesatti [Part I]

fig. 6

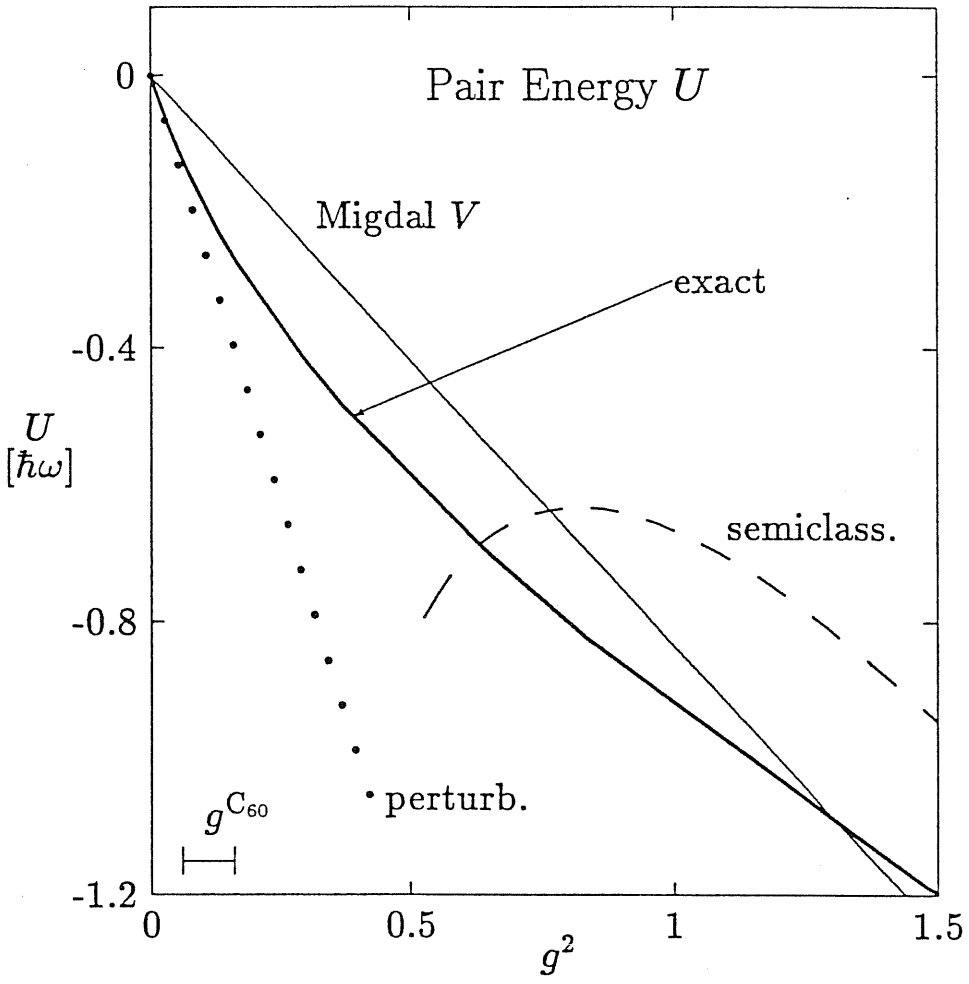

Auerbach Manini Tosatti [Part I]

fig 7

Electron–Vibron Interactions in Charged Buckminsterfullerene: Pair Energies and Spectra (Part II)

Nicola Manini[a]*, Erio Tosatti[a,b]†,
a) International School for Advanced Studies (SISSA), via Beirut 2-4, I-34013 Trieste, Italy,
b) International Centre for Theoretical Physics (ICTP), P.O. BOX 586, I-34014 Trieste, Italy,
and
Assa Auerbach‡
Physics Department, Technion, Haifa, Israel.

January 12, 1994

Abstract

The ground state energy shifts and excitation spectra of charged buckminsterfullerene C_{60}^{n-}, $n = 1, \ldots 5$ are calculated. The electron–vibron Hamiltonian of Part I is extended to include all A_g and H_g modes with experimentally determined frequencies and theoretically estimated coupling constants. Complex splitting patterns of H_g vibrational levels are found. Our results are relevant to EPR measurements of spin splittings in C_{60}^{2-} and C_{60}^{3-} in solution. Spectroscopic gas-phase experiments will be of interest for further testing of this theory. As found in Part I, degeneracies in the electron and vibron Hamiltonians give rise to a dynamical Jahn Teller effect, and to a considerable

*Email: manini@tsmi19.sissa.it
†Email: tosatti@tsmi19.sissa.it
‡Email: assa@phassa.technion.ac.il

SISSA REF: 5/94/CM/MB

enhancement of the electronic pairing interaction. This helps to overcome repulsive Coulomb interactions and has important implications for superconductivity in K_3C_{60} and the insulating state in K_4C_{60}.

PACS: 31.30,33.10.Lb,33.20.E,33.20.F,71.38.+i,74.20.-z,74.70.W

1 Introduction

This paper continues the investigations of the electron-vibron interactions within a fullerene molecular anion, C_{60}^{n-}. In Part I (Ref. [1]) we considered in great detail the idealized case of a single H_g vibron mode coupled to the electronic degenerate t_{1u} orbital for n=1,..5 electrons. By solving the problem for strong, intermediate and weak coupling regimes, we have shown the existence of Berry phases for odd n, and their importance in determining ground state energies and degeneracies. The Berry phase effects are clearest in strong coupling, where the parity of the pseudorotational orbital angular momentum L, is related to the electron filling n by

$$(-1)^{L+n} = 1 \tag{1}$$

The effects on the energies however are relatively stronger in weak coupling where quantum corrections enhance pair binding which is a factor $5/2$ *larger* than the corresponding classical Jahn-Teller (JT) relaxation energy E^{JT}. This leads to larger electron-vibron pairing interaction than previously calculated using Migdal-Eliashberg theory. Moreover, this enhancement is of direct importance to C_{60}^{n-}, where the electron-vibron coupling is weak to intermediate. These encouraging results clearly call for a more realistic study of the full electron-vibron problem of C_{60}^{n-}. This is the purpose of this paper, where we will address both the vibronic spectrum, and the pairing energies, in quantitative detail.

The full molecular Hamiltonian describes the dynamics of 60 carbon atoms plus $240+n$ valence electrons. The problem is substantially simpli-

fied by assuming the knowledge of the non interacting spectra for electronic levels [2, 3, 4] and for molecular vibrations, both from theory [3, 4] and experiment [5, 6]. For n=0, the electrons form a closed shell. This allows a Born-Oppenheimer decoupling of the vibron and electron systems. For n=1,...5, however, the extra electrons partly fill the threefold degenerate Lowest Unoccupied Molecular Orbitals (LUMO) states of t_{1u} symmetry, which gives rise to a linearly coupled JT system. Other orbitals, such as the Highest Occupied Molecular Orbitals (HOMO) states of h_u symmetry, at ~ -2eV below the LUMO states, and the t_{2g} (LUMO+1) states at $\sim +1$eV, introduce weaker quadratic electron-vibron couplings which we presently ignore. Further complications may arise from anharmonic effects.

Fortunately, neglect of all these higher order effects is expected to be a very good approximation in C_{60}^{n-}, where the t_{1u} level is very well separated from others, and the C-C bonds are rather stiff and harmonic. Detailed Hartree-Fock calculations have shown, for example, that the energy gain by going from I_h to D_{5d}, D_{3d}, D_{2h} symmetries via static JT distortions, are in fact identical to within 1% [7]. Therefore, restricting to the t_{1u} orbital, to linear JT coupling and harmonic vibrons is very well justified in C_{60}^{n-}. Neglecting also Coulomb interactions (they will be discussed separately in Section 3), the full electronic problem is therefore replaced by a 3×3 matrix linearly coupled to vibrons.

Thus our Hamiltonian is an extension of the single mode mode solved in full in Part I. Here we shall include the eight H_g vibron modes of real C_{60}, instead of only one. Also we shall include two A_g vibrons which also couple linearly to the LUMO electrons, even though they do not split its degeneracy. Symmetry prevents all other vibrons different from A_g and H_g to interact linearly with the t_{1u} orbitals. If we further neglect higher order interactions, all other vibrons are decoupled and unaffected by changing the electronic filling n.

Generally speaking, even with these drastic approximations, a realistic

description of the dynamical JT state of a C_{60}^{n-} ion is a more complicated affair than the single mode treated in Part I. For a general coupling strength, there is in fact no linear superposition between effects produced by different H_g vibrons coupled to the *same* t_{1u} orbital. Luckily, however, linear superposition turns out to be valid in the weak coupling perturbative regime, which, in turn, applies, even if only approximately, to fullerene.

In this paper we apply perturbation theory to the full electron-vibron problem of C_{60}^{n-}, with n=1 to 5 in a t_{1u} orbital, and including all A_g and H_g modes [8]. As in Part I, we make the further approximation of replacing a spherically symmetrical coupling to the true icosahedral hamiltonian on the C_{60} ball. Analytical expressions correct to second order in the electron-vibron coupling strengths are found for ground state and excitation energies, as well as for electron pair binding energies ("effective Hubbard U's"). Using realistic coupling constants from Local Density Approximation calculations, we obtain numerical estimates for these vibron-induced pair energies and find them to be unexpectedly large and negative (≈ -0.2eV) for n=1,3,5, and even larger but positive (≈ 0.4eV) for n=2,4. This finding is discussed in qualitative connection with superconductivity in A_3C_{60} [9, 10, 11], and with the insulating state of A_4C_{60} (A=K,Rb).

The calculated vibron spectrum of C_{60}^{n-} is also presented in detail. Notwithstanding the uncertainty in the physical coupling constants, large splittings of all H_g modes are predicted. These are expected to be observable for example in gas phase C_{60}^{-} and C_{60}^{2-} ions. This part is organized as follows: Section 2 defines the multi vibron model. Section 3 describes the perturbative calculation of the spectrum. Section 4 presents the relation of the results to experimental measurements of vibron spectroscopy of C_{60}^{n-} anions. Section 5 discusses the interplay between electron-vibron and Coulomb interactions for the ground state and pair binding energies. We conclude with a short summary.

2 The Hamiltonian

The single electron LUMO states of C_{60} are in a triplet of t_{1u} representation. The important vibrational modes which couple to this electronic shell are of two representations: A_g (one dimensional) and H_g (five dimensional). A_g, t_{1u} and H_g are the icosahedral group counterparts of the spherical harmonics 1, $\{Y_{1m}\}_{m=-1}^{1}$, and $\{Y_{2m}\}_{m=-2}^{2}$ respectively. By replacing the truncated icosahedron (soccer ball) by a sphere, we ignore lattice corrugation effects which are expected to be small for the electron-vibron interactions, since they do not lift the degeneracies of $L = 0, 1, 2$ representations.

The Hamiltonian includes the terms

$$H = H^0 + H^{e-v} + \cdots \tag{2}$$

where electron-electron interactions, anharmonic interactions between phonon modes, and anharmonic coupling terms have been neglected. The non interacting Hamiltonian is

$$H^0 = \hbar \sum_k \omega_k \sum_{M=-L_k,L_k} \left(b^\dagger_{kM} b_{kM} + \frac{1}{2} \right) + (\epsilon - \mu) \sum_{ms} c^\dagger_{ms} c_{ms}, \tag{3}$$

$b^\dagger_{kM}$ creates a vibron of mode k and energy ω_k in the spherical harmonic state Y_{L_kM}, where L_k denotes the angular momentum of mode k, either 0 or 2 according to whether k is an A_g or an H_g representation respectively. $c^\dagger_{ms}$ creates an electron of spin s in an orbital Y_{1m}. This Hamiltonian operates on the basis

$$\prod_{KM} |n_{kM}\rangle_v \prod_{ms} |n_{ms}\rangle_e \tag{4}$$

where $|n_{kM}\rangle_v$ ($|n_{ms}\rangle_e$) is a vibron (electron) Fock state. By setting $\mu \to \epsilon$ we discard the second term in (3).

The electron–vibron interaction is local and we assume it to be rotationally invariant. The nuclear vibration field of eigenvector k is

$$u_k(\hat{\Omega}) = \sum_M \frac{1}{\sqrt{2}} (Y^*_{L_kM}(\hat{\Omega}) b^\dagger_{L_kMk} + Y_{L_kM}(\hat{\Omega}) b_{L_kMk}) \tag{5}$$

where $\hat{\Omega}$ is a unit vector on the sphere. The interaction between the vibrations and electron density is

$$H^{e-v} \propto \sum_k g_k \int d\hat{\Omega}\; u_k(\hat{\Omega}) \sum_s \psi_s^\dagger(\hat{\Omega})\psi_s(\hat{\Omega}) \tag{6}$$

where the electron field operators are

$$\psi_s(\hat{\Omega}) = \sum_{m=-1}^{1} Y_{1m}(\hat{\Omega}) c_{ms} \tag{7}$$

Using the relation

$$\int d\hat{\Omega}\; Y_{LM}(\hat{\Omega}) Y_{lm_1}(\hat{\Omega}) Y_{lm_2}(\hat{\Omega}) \propto (-1)^M \langle L, -M | lm_1; lm_2 \rangle, \tag{8}$$

where $\langle \cdots \rangle$ is a Clebsch-Gordan coefficient [12], yields the second quantized Hamiltonian

$$\begin{aligned}
H^{e-v} &= H_{A_g}^{e-v} + H_{H_g}^{e-v} \\
H_{A_g}^{e-v} &= \sqrt{\frac{3}{2}}\hbar \sum_{k=1}^{2} g_k \omega_k \sum_{ms} (-1)^m \left(b_{k0}^\dagger + b_{k0} \right) \\
&\qquad \times \langle 0,0 | 1,-m; 1,m \rangle c_{ms}^\dagger c_{ms} \\
H_{H_g}^{e-v} &= \frac{\sqrt{3}}{2}\hbar \sum_{k=3}^{10} g_k \omega_k \sum_{M=-2}^{2} \sum_{ms} (-1)^m \left(b_{kM}^\dagger + (-1)^M b_{k\,-M} \right) \\
&\qquad \times \langle 2, M | 1, -m; 1, m+M \rangle c_{ms}^\dagger c_{m+M\,s} \;,
\end{aligned} \tag{9}$$

where the numerical constants are fixed by the requirement that the classical JT energy gain of a single mode k is $g_k^2/2$ [1].

3 The Multi–Mode Spectrum (Weak Coupling)

The perturbation hamiltonian (9) written in the Fock basis (4), connects states whose number of vibrons $N_v(k)$ of mode k differs by exactly ± 1. Thus,

first order corrections to the energies vanish. Second order corrections are obtained by diagonalizing the matrix [13]

$$\Delta^{(2)}_{a,b} = \langle a|H^{e-v}\frac{1}{E^{(0)}_a - H^0}H^{e-v}|b\rangle, \qquad (10)$$

where $|a\rangle$ and $|b\rangle$ are members of the same degenerate manifold, i.e. they have the same number of vibrons $N_v(k)$. The sum implied by the inverse operator $(E^{(0)}_a - H^0)^{-1}$ extends just to those states whose N_v's differ only by ± 1 from that of the multiplet being perturbed. This means that to second order in the coupling constants g_k there are no direct inter-mode interactions, and the modes can be treated separately. The only second-order inter-mode coupling is a consequence of all the modes having a common ground state (N_v=0). The effect of vibron k affects this N_v=0 state either with a pure shift or through both shift and splitting. However all other modes k', having their ladder built on the same N_v=0 state, are shifted or split by vibron k, according to the same structure of this N_v=0 multiplet. This effect takes place through additive contributions proportional to g_k^2 to the diagonal matrix elements $\Delta^{(2)}_{a,a}$ relative to the k' ladder, without involving off-diagonal inter-mode couplings, which would be related to g^4 and higher order corrections.

A single A_g mode coupled to a t_{1u} level is the simple polaron problem, which is exactly soluble [14]: the second order energy is exact. Since the A_g representation is one-dimensional, it does not split the electronic degeneracy. The only effect is a downward shift of the whole spectrum. The amount of A_g-related energy shift is found to be $-E_k^{JT}$, $-4E_k^{JT}$ and $-6E_k^{JT}$, for n=1, 2 and 3 respectively (where E_k^{JT} is the classical JT energy gain $\equiv g_k^2\hbar\omega_k/2$ of that mode $A_g(k)$). Obviously, these results hold for both unpolarized and polarized spin states, since the t_{1u} levels remain degenerate.

For the H_g modes the situation is more complicated. For n=1, the degenerate vibronic t_{1u} ground state is not split by JT coupling, as it conserves its L=1 symmetry. For this reason, the only contribution of the vibron $H_g(k)$ to the spectrum of another vibron $H_g(k')$ is just a constant energy shift of

-5/4 g_k^2, which obviously does not affect *energy differences* in the spectrum of vibron k'. This is perfectly analogous to the effect of a single A_g mode on all the other vibrons.

By contrast, the n=2,4 and n=3 lowest vibronic multiplets (N_v=0) are split (into ^{1}S, ^{1}D, ^{3}P, and ^{2}P, ^{2}D, ^{4}S levels respectively). Correspondingly, the levels of an interacting vibron k receive different diagonal contributions of order $g_{k'}^2$ from different interacting vibrons k', giving rise to a more intricate pattern of splittings.

For the sake of simplicity, and also since C_{60}^- seems easiest to obtain in the gas phase [15], we will concentrate on the many-modes spectrum for n=1. The perturbative results for all H_g and A_g modes will be presented in Section 4. In principle, the full spectra for n=2,3,4, can be determined following the same method.

The spectrum for a single H_g mode is given in Table I for the degenerate multiplets N_v=0 and N_v=1, and for n=1, 2, (S=0) and 3 (S=1/2) electrons. In Figures (1, 2, 3) we replot on an expanded scale the results of exact diagonalization of Ref [1] for 1, 2 and 3 electrons, along with the straight lines corresponding to present perturbative results for the lowest few states. These figures confirm that perturbative results retain quantitative validity up to $g \approx 0.3$. In the special case n=1, moreover, the perturbative results lay within $0.05\hbar\omega$ of the exact value up to $g \leq 0.4$.

We have therefore an approximate analytical estimate of the splittings induced by JT coupling, valid in weak coupling. For example, for n=1 the H_g vibron excitation, originally at energy 1 above the ground state, splits into three vibronic levels with relative shifts $-\frac{3}{4}g^2$, $\frac{3}{8}g^2$ and $\frac{9}{8}g^2$ (in units of $\hbar\omega$ of that vibron). Table I contains the complete list of these low lying excitations energies, accurate to order g^2.

Because the effects of all A_g and H_g modes can be linearly superposed, there are two ingredients only, which we need to have in order to transform the analytical shifts of Table I into actual numbers for C_{60}^{n-}: the frequencies

$\hbar\omega_k$ and the coupling constants g_k of each individual H_g and A_g mode. For the frequencies, there are both calculated and measured values. We can avoid uncertainties by choosing the latter as given, e.g. for neutral C_{60} in Ref.[6]. In doing so, we neglect the well known small systematic frequency shifts associated with bond-length readjustments and other electronic effects going from C_{60} to C_{60}^{n-} [16, 17]. They also depend on the environment of the C_{60}^{n-} ion.

There are several calculated sets of coupling constants g_k [3, 10, 9, 18], but no direct measurement. Since the agreement among the different calculations is far from good, in Section 4 we present the results of several selected sets, which provides an estimate of the relevant uncertainties. We will eventually adopt the most recent values of Antropov *et al.* [18].

As seen in Table II, almost all of the couplings g_k are weak, $g_k \leq 0.4$. As discussed, in this range the perturbative results are accurate within ten per cent or better for all the low lying states. As the discrepancies among the various estimates of the g_i is much larger, these perturbative formulas are at this stage more than adequate, and particularly good in the n=1 case, where the distortion is smallest.

This is fortunate, since exact diagonalization is computationally rather demanding if all H_g modes are included. Better knowledge of frequencies and coupling constants might warrant a calculation of higher orders in g_k.

4 Vibron spectroscopy of C_{60}^{n-} anions.

The electron affinity of C_{60} is large (2.7 eV) and experimental evidence has been found that the C_{60}^{-} [15] and C_{60}^{2-} [19] are stable ions in vacuum. In solution a wider spectrum of ionization states has been demonstrated electrochemically, up to and including C_{60}^{5-} [20, 21, 22]. As an adsorbate on a metal surface, the electronegative C_{60} molecule naturally picks up electrons [23, 24], and recent evidence has been provided of charge transfer which can

be as large as n=6 [17]. In the solid state, finally, there are compounds, covering a wide range of charge transfers, from n=1, as in $TDAE^{+}$-C_{60}^{-} [25] or Rb_1C_{60} [26], n=3, as in K_3C_{60} or Rb_3C_{60} [27], n=4 as in K_4C_{60} [28], n=6 as in Rb_6C_{60} [29], or even higher as in $Li_{12}C_{60}$ [30, 16].

Among these systems, our calculations so far address concretely only the gas phase case. Unfortunately, to our knowledge no investigation appears to have been made of the vibrational excitations of isolated C_{60}^{-} and C_{60}^{2-}. Our calculated excitation spectrum for C_{60}^{-} therefore constitutes a prediction which we hope will stimulate new work.

In Table II we report the excitation energies predicted by perturbation theory, applied to the eight modes in the C_{60}^{-} case. Selection rules are not discussed here for any particular spectroscopy. We simply give the symmetry assignments.

As is seen, the predicted splittings due to dynamical JT coupling are generally quite large, and should be well observed spectroscopically. However, as indicated by comparison between different sets of g_k's, there is a large uncertainty in these predicted splittings of the same order of magnitude as the splittings themselves. As remarked earlier, the same uncertainty does not affect the energetics of the following section, which is on safer grounds. Our calculated spectrum is therefore of qualitative value, and we rather expect it to work backwards. That is, a future precise measurement of the splittings should provide an accurate evaluation of the actual couplings.

As a further caution, we should stress that our spherical representations in the Hamiltonian (9) neglect interactions due to the icosahedral lattice of carbons. For example the vibron multiplet of $L = 3$ decomposes due to the lattice into $T_{2u} \oplus G_u$ [31] , etc. In addition to neglecting lattice effects and anharmonic interactions, we also ignore spin-orbit coupling. As remarked in Part I, it has been shown [32] to yield splittings of the order of 50 cm^{-1} to the L =1 ground state (in Ar matrix), which is not a negligible amount. Thus we estimate that the splittings obtained by our Hamiltonian should dominate

the splittings found in the real spectrum.

As pointed out by Bergomi and Jolicoeur [33], experiments on anions in matrix may be relevant to the vibronic effects. Near infrared and optical spectra of C_{60}^{n-} ions in solution are available [21]. A major $t_{1u} \rightarrow t_{1g}$ optical transition near 1 eV is present for all n values. It is accompanied by additional vibronic shake-up structures, typically near 350, 750, 1400 and 1600 cm^{-1}. This limited information seems as yet insufficient for any relevant comparison with our calculations. Well defined vibrational spectra are instead available for chemisorbed C_{60}^{n-} [17] and for A_nC_{60} alkali fullerides [29]. In this case, however, interaction of the electronic t_{1u} level with surface states or with other t_{1u} states of neighbouring balls must turn the level into a broad band, and our treatment as it stands is invalid. One can generally expect rapid electron hopping from a molecule to another to interfere substantially with the dynamical JT process, in a way which is not known at present. The spectra of charged C_{60} adsorbates and solids, in any case, do not present evidence of any dynamic splittings such as those of Table II, but rather of a gradual continuous shift most likely due to a gradual overall change of geometry, as suggested also by LDA calculations [4].

Summarizing, we are yet unaware of detailed spectroscopic confirmation of the electron-vibron effects. We expect however these effects to be observable in the gas phase of C_{60}^{-} and C_{60}^{2-}. In particular for C_{60}^{-} an observation that the lowest H_g vibron splits into a near 7-fold degenerate multiplet (i.e. from the $L = 3 \equiv T_{2u} \oplus G_u$ pseudorotation level) would be an important confirmation of the electron vibron theory and effects of Berry phases.

5 Ground state energetics and effective Hubbard U's.

Perturbation theory allows us to write analytic expressions for the energy gain of the ground state at different n, and therefore for the pair energy

$$U_n = E_{n+1} + E_{n-1} - 2E_n \ , \tag{11}$$

as discussed in Ref [1]. Comparison with exact single-mode results shows a systematical perturbative overestimate (Figures 1, 2, 3) of the H_g-related ground state energy shift. The error is however relatively small and quite acceptable for the couplings in Table II. The shift is 5/2 times larger than its classical value, as discussed in Ref. [1]. This factor 5/2 is important, because it leads in turn to a surprisingly large energetic lowering even for small g's, making JT vibronic coupling a much more important affair than it was understood so far. The physical reason for the large energy gain is that the dynamically JT distorted molecule undergoes a dramatic decrease of vibrational zero-point energy. This adds an extra $-\frac{3}{4}g^2\hbar\omega$ (in the n=1 case, say) to the *static* JT gain $-\frac{1}{2}g^2\hbar\omega$ of each H_g mode. The zero-point energy decreases faster at small g probably because the mexican-hat potential well is more "square-well"-like than the original harmonic potential. We also note that the proliferation of excited states upon coupling H_g with t_{1u} is of fermionic origin, and does not add to the zero-point energy.

Within second order perturbation theory the ground state energy is a sum of all the 2+8 contributions of the $A_g + H_g$ modes:

$$E_{tot}(n) = E_{A_g} + E_{H_g} = a_n E^{JT}_{A_g} + b_n E^{JT}_{H_g} = a_n \sum_{k=1}^{2} E^{JT}_k + b_n \sum_{k=3}^{10} E^{JT}_k \ , \tag{12}$$

where

$$E^{JT}_k \equiv \frac{1}{2} g_k^2 \hbar\omega_k, \tag{13}$$

We already discussed in Section 3 the JT ground state energy gains due to an A_g mode, with coefficients a_n=-1, -4, and -6, for n=1, 2 and 3 respectively. Table I gives the corresponding energies for the $H_g(k)$ modes ($k > 2$). These are given by

$$\begin{array}{ll} -\frac{5}{2}E_{2\,k}^{JT} & n=1 \\ -10E_{2\,k}^{JT} & n=2 \\ -\frac{15}{2}E_{2\,k}^{JT} & n=3 \end{array} \qquad (14)$$

the appropriate coefficients being therefore b_1=-5/2, b_2=-10, b_3=-15/2.

These expressions allow us to compute the individual contribution to the pair energies U_n (Eq. (11)) due to the A_g and H_g modes. We give these formulae in Table III. The corresponding numerical values are reported in Table IV, based on the ground state energy gains as given by the set of coupling constants of Eq. (11).

We consider the unpolarized spin sector. Similar subtractions could easily be done, if needed, for high-spin states, or high- and low-spin, using, for example $E_{tot}(n{=}2,S{=}0)$, with $E_{tot}(n{=}3,S{=}3/2)$. Although, as we pointed out, the values of the individual g_k's of Ref. [18], [10] and [9] are significantly uncertain, the global E_{H_g} is much less author-dependent, amounting to 102 meV, 84 meV and 78 meV respectively (n=1).

As Table II shows, the coupling with the A_g mode pushes U_1 further towards negative values, but has the opposite effect on U_2 and U_3.

The overall enhancement factor 5/2 in the ground state H_g shift ends up producing a much larger pair energy than expected so far based on classical JT energies [9]. In particular, our calculated JT energy gain of $\approx$ 0.4 eV for n=2 and $\approx$ 0.3 eV for n=3 (low-spin) is almost one order of magnitude larger than the currently accepted values! This has important implications, first of all, in determining whether the simple C_{60}^{n-} ion, in vacuum, in a matrix or in solution, will choose to be high-spin or low-spin.

In order to discuss this point, we recall the existence of an intra-ball Coulomb repulsion **U** (not to be confused with the pair energy of Ref [1]), which for a t_{1u} level is a matrix, specified by two main values, $U_{||}$ (two electrons in the same orbital), and $U_{\perp} < U_{||}$ (two electrons in different orbitals). Using the JT energy differences between the high- and low-spin states as

$$\begin{aligned} E^{(2)}_{S=0} - E^{(2)}_{S=1} &= (U^{(2)}_{||} - 4E^{JT}_{A_g} - 10E^{JT}_{H_g}) - (U^{(2)}_{\perp} - 4E^{JT}_{A_g} - \frac{5}{2}E^{JT}_{H_g}) \\ &= (U^{(2)}_{||} - U^{(2)}_{\perp}) - \frac{15}{2}E^{JT}_{H_g} \approx (U^{(2)}_{||} - U^{(2)}_{\perp}) - 0.3eV \quad (15) \\ E^{(3)}_{S=\frac{1}{2}} - E^{(3)}_{S=\frac{3}{2}} &= (U^{(3)}_{||} + 2U^{(3)}_{\perp} - 6E^{JT}_{A_g} - \frac{15}{2}E^{JT}_{H_g}) - (3U^{(3)}_{\perp} - 6E^{JT}_{A_g}) \\ &= (U^{(3)}_{||} - U^{(3)}_{\perp}) - \frac{15}{2}E^{JT}_{H_g} \approx (U^{(3)}_{||} - U^{(3)}_{\perp}) - 0.3eV \ , \quad (16) \end{aligned}$$

where we have used the fact that the JT energetics for n=2, S=1 is identical to that for n=1, S=1/2 [1], while for n=3, S=3/2 there is no JT distortion. We have also used the t_{1u} orbital unimodal and bimodal splitting patterns of Part I to identify the filling (n_1, n_2, n_3). In particular the fillings assumed are (0,0,2) for n=2, S=0; (1,1,0) for n=2, S=1; (0,1,2) for n=3, S=1/2; (1,1,1) for n=3, S=3/2.

So long as $\mathbf{U}^{(n)}$ may be expected to vary slowly with the electron number n, then the two energy differences (15) and (16) should be very similar. Moreover, the prevailing of a high- or of a low-spin state is decided by a fine balance between the Coulomb repulsion anisotropy $(U_{||} - U_{\perp})$ and the dynamical JT gain $\frac{15}{2}E^{JT}_{H_g}$ This suggests the possibility that if high-spin is more likely to prevail for C_{60}^{2-} and C_{60}^{3-} in the gas phase, where **U** is large, the balance might easily reverse in favor of low-spin when in matrix or in solution. Recent EPR data indicate that this is precisely the case. When frozen in a CH_2Cl_2 glass, C_{60}^{2-} appears to be in a high-spin, S=1 state [20]. Hence, in this case $(U_{||} - U_{\perp})$ is larger than 0.3 eV. However, optical and EPR data for C_{60}^{3-} in CH_2Cl_2 and other matrices favor a low-spin state [21]. Now $U^{(3)}_{||} - U^{(3)}_{\perp}$ has therefore become smaller than 0.3 eV. We can conclude that,

even for a single embedded molecule, the *balance between intra-ball Coulomb repulsion and dynamical JT energy gains is extremely critical.*

Recent photoemission and Auger data [34] have shown that the intra h_u HOMO orbital Coulomb U is not as large as it was previously supposed. In particular, a decrease by only 0.23 eV from gas phase C_{60} and the crystalline C_{60} hole-hole Auger shifts, implies $|U| < 1$ eV in the latter. This upper bound is about a factor three smaller than those previously proposed [35]. In the light of this observation, it is not at all surprising to find that $U_{||} - U_{\perp}$ is in the neighbourhood of 0.3 eV for C_{60}^{n-} in a matrix.

Coming next to the pair binding energies of Ref [1], we find large negative dynamical JT-related U_n's for odd n. Even if we omit the A_g contribution (which may be irrelevant for superconductivity, due to screening [18]), we get U_3=-0.2 eV. This negative value, will cancel at least a good fraction of the Coulomb positive intra-ball pair energy

$$U_3^{Coul} = U_{||}^{(2)} + (2U_{||}^{(4)} + 4U_{\perp}^{(4)}) - 2(U_{||}^{(3)} + 2U_{\perp}^{(3)}) \approx U_{||} \qquad (17)$$

This cancellation implies a severe decrease of the Coulomb pseudopotential μ^* relative to that calculated when the JT coupling is ignored [36]. For a sufficiently strong solid-state screening of the electronic $U_{||}$ and $U_{\perp}$, it may well be sufficient to reverse to a negative μ^*, i.e. to an overall negative Hubbard U state.

For n=2 and 4, dynamical JT stabilizes the average configuration of C_{60}^{n-}, since the pair energy is *positive*: $U_2 \approx 0.4$ eV. This now acts to reinforce the bare Coulomb pair energy

$$U_2^{Coul} = U_{||}^{(3)} - 2U_{\perp}^{(3)} - 2U_{||}^{(2)} \approx 2U_{\perp} - U_{||}$$

$$U_4^{Coul} = (2U_{||}^{(5)} + 8U_{\perp}^{(5)}) + (U_{||}^{(3)} + 2U_{\perp}^{(3)}) - 2(2U_{||}^{(4)} + 4U_{\perp}^{(4)}) \approx 2U_{\perp} - U_{||} \qquad (18)$$

where a filling (2,2,1) has been assumed for n=5.

For even n, the JT coupling stabilizes a *correlated insulating state* of a lattice of evenly-charged C_{60} molecules. In this type of insulator, fluctuations

about $\langle n_i \rangle = n$ are suppressed, and a gap of order U_n is opened in the electronic spectrum.

This state has an even number of electrons per site, and is non-magnetic, very much like a regular band insulator. However, electron correlations responsible for band narrowing and gap opening are *vibronic* in origin. We suggest that the (body-centered tetragonal [37]) structure of K_4C_{60} and Rb_4C_{60} may be a realization of this state where electronic and vibronic interactions play an important role. So far, band calculations [23] and experiments [38] had been in disagreement, the former suggesting a metal, and the latter finding a narrow-gap insulator.

Very recent UPS data on K_nC_{60} [40] have shown a *decrease* of the energy difference between the HOMO and the Fermi level (inside the t_{1u} LUMO) when going from n=3 to n=4 and finally to n=6. This kind of non-rigid band behaviour is in itself not a surprising result. The surprise is that the decrease is very large from n=3 to n=4 ($\approx$ 0.4 eV), and smaller from n=4 to n=6 ($\approx$ 0.2 eV). As pointed out by De Seta and Evangelisti, a positive Coulomb U would predict exactly the opposite. We observe that this behaviour is instead in agreement with our predicted pattern of effective U_n of vibronic origin, which is therefore supported by these data.

Additional experiments which may probe the electron–vibron interactions are short time resolved spectroscopy of excitons in neutral C_{60} [39]. An exciton consists of an electron in the LUMO orbital and a hole in the H_g HOMO levels, which interact with different strengths with the vibrons. The hole-vibron coupling inside the HOMO could be studied along similar lines to those presented above for the t_{1u} LUMO.

As for superconductivity in solids with n=3, we expect the enhanced pair binding found here to be crucial for overcoming the on-site Coulomb repulsion and for enhancing T_c over its value in, e.g., graphite intercalates. Broadening of the t_{1u} electron level into a band of non-negligible width makes the present treatment insufficient for quantitative predictions. From the fundamental

point of view however, it is amusing to note that superconductivity can be enhanced by a decrease of *lattice zero-point* energy. This adds to the usual BCS mechanism of reducing the electron *kinetic* energy by opening a gap. We hope to pursue this line of thought further in future work.

6 Summary

In conclusion, a full treatment of all the A_g and H_g modes has been given, and shown to yield analytical results with quantitative accuracy for the full dynamical JT problem of C_{60}^{n-}. The ground state energetics has been studied, and unexpectedly large energy gains have been found, due to a decrease of zero-point energy. This implies large positive effective U_n for n=2 and 4, and a large negative U_3, which is very interesting in view of superconductivity in K_3C_{60} and insulating behaviour in K_4C_{60}. Detailed vibrational spectra for C_{60}^{n-} are presented, and proposed for spectroscopic investigation, particularly in gas phase.

Related work is also being done by other groups [41].

Acknowledgements

ET and NM wish to acknowledge discussions with W. Andreoni, E. Burstein, J. Kohanoff, S. Modesti, L. Pietronero, P. Rudolf, C. Taliani and L. Yu. A.A. thanks Mary O'Brien, Art Hebard and Zeev Vardeny for valuable discussions, and acknowledges the Sloan Foundation for a fellowship. This paper was supported by grants from the US-Israel Binational Science Foundation, the Fund for Promotion of Research at the Technion, and the US Department of Energy No. DE-FG02-91ER45441, the Italian Istituto Nazionale di Fisica della Materia INFM, the European US Army Research Office, and NATO through CRG 920828.

References

[1] A. Auerbach, N. Manini and E. Tosatti, Phys. Rev. B, preceding paper.

[2] R. C. Haddon, L. E. Brus, and K. Raghavachari, Chem. Phys. Lett. **125**, 459 (1986); S. Satpathy, Chem. Phys. Lett. **130**, 545 (1986).

[3] F. Negri, G. Orlandi, F. Zerbetto, Chem. Phys. Lett. **144**, 31 (1988).

[4] B. P. Feuston, W. Andreoni, M. Parrinello, and E. Clementi, Phys. Rev. B. **44** 4056 (1991); J. Kohanoff, W. Andreoni, and M. Parrinello, Phys. Rev. B. **46** 4371 (1992).

[5] K. Prassides, T. J. S. Dennis, J. P. Hare, J. Tomkinson, H. W. Kroto, R. Taylor, and D. R. M. Walton Chem. Phys. Lett. **187**, 455 (1991); R. A. Jishi, M. S. Dresselhaus, Phys. Rev. B **45**, 2597 (1992); M. G. Mitch, S. J. Chase, and J. S. Lannin, Phys. Rev. B **46** 3696 (1992).

[6] P. Zhou K. A. Wang, Y. Wang, P. C. Eklund, M. S. Dresselhaus, G. Dresselhaus, and R. A. Jishi, Phys. Rev. B **46**, 2595 (1992).

[7] N. Koga and K. Morokuma, Chem. Phys. Lett. **196**, 191 (1992).

[8] Because of electron-hole symmetry, fillings n and 6-n are equivalent, leaving n=1, 2, 3 as the only inequivalent states.

[9] M. Schlüter, M. Lannoo, M. Needels, G. A. Baraff, and D. Tománek, Phys. Rev. Lett.**68**, 526 (1991); J. Phys. Chem. Solids, **53**, 1473 (1992).

[10] C. M. Varma, J. Zaanen, and K. Raghavachari, Science, **254**, 989 (1991).

[11] An earlier suggestion of a connection between dynamical JT effect and fullerene superconductivity was made by K. H. Johnson, M. E. McHenry and D. P. Clougherty, Physica C **183**, 319 (1991).

[12] A. R. Edmonds, *Angular Momentum In Quantum Mechanics*, (Princeton University Press, Princeton, 1974).

[13] J. J. Sakurai, *Modern Quantum Mechanics*, (Benjamin, Menlo Park, Calif., 1985).

[14] G. D. Mahan, *Many-Partical Physics* (Plenum, New York, 1981).

[15] S. H. Yang C. L. Pettiette, J. Conceicao, O. Cheshnovsky, and R. E. Smalley, Chem. Phys. Lett. **139**, 233 (1987).

[16] J. Kohanoff, W. Andreoni, and M. Parrinello Chem. Phys. Lett. **198**, 472 (1992); J. Kohanoff, Thesis, ETH N.10079 (1993); W. Andreoni, in *Electronic Properties of New Materials: Fullerenes*, Proceedings of the Kirchberg Winter School, edited by H. Kuzmany, J. Fink, M. Mehring and S. Roth, March 6-11, 1993 (Springer Verlag, in press).

[17] S. Modesti, S. Cerasari, and P. Rudolf, Phys. Rev. Lett. **71**, 2469 (1993).

[18] V. P. Antropov, A. Gunnarsson, and A. I. Liechtenstein, Phys. Rev. B **48**, 7651 (1993).

[19] P. A. Limbach, L. Schweikhard, K. A. Cowen, M. T. McDermott, A. G. Marshall, and J. V. Coe, J. Am. Chem. Soc. **113**, 6795 (1991).

[20] D. Dubois, K. M. Kadish, S. Flanagan, R. R. Haufler, L. P. F. Chibante, and L. J. Wilson, J. Am. Chem. Soc. **113**, 4364 (1991).

[21] G. A. Heath, J. E. McGrady, and R. L. Martin, J. Chem. Soc., Chem. Commun. 1272 (1992); P. Bhyrappa, P. Paul, J. Stinchcombe, P. D. W. Boyd, and C. A. Reed, J. Am. Chem. Soc. **115**, 11004 (1993), and references therein.

[22] W. K. Fullagar, I. R. Gentle, G. A. Heath, and J. W. White, J. Chem. Soc., Chem. Commun. 525 (1993).

[23] S. C. Erwin in *Buckminsterfullerenes*, edited by W. E. Billups and M. A. Ciufolini (VCH Publishers, New York, 1993), p. 217; we are grateful to Dr. W. Andereoni for pointing out this reference to us.

[24] E. Burstein, S. C. Erwin, M. Y. Jiang, and R. P. Messmer, Physica Scripta **T42**, 207 (1992).

[25] V. N. Denisov, A. A. Zakhidov, G. Ruani, R. Zamboni, C. Taliani, K. Tanaka, K. Yoshizawa, T. Okahara, T. Yamabe, and Y. Achiba, Synth. Metals **55-57**, 3050 (1993).

[26] P. J. Benning, F. Stepniak, and J.H. Weaver, Phys. Rev. B **48**, 9086 (1993).

[27] A. F. Hebard, Phys. Today, Nov. 1992, p. 26, and references therein.

[28] R. F. Kiefl, T. L. Duty, J. W. Schneider, A. MacFarlane, K. Chow, J. W. Elzey, P. Mendels, G. D. Morris, J. H. Brewer, E. J. Ansaldo, C. Niedermayer, D. R. Noakes, C. E. Stronach, B. Hitti, and J. E. Fischer, Phys. Rev. Lett. **69**, 2005 (1992).

[29] J. E. Fischer and P. A. Heiney, J. Phys. Chem. Solids (to be published) (1993), and references therein.

[30] Y. Chabre, D. Djurado, M. Armand, W. R. Romanons, N. Coustel, J. P. McCauley Jr, J. E. Fischer, and A. B. Smith III, J. Am. Chem. Soc. **114**, 764 (1992).

[31] M. Ozaki, and A. Takahashi, Chem. Phys. Lett. **127**, 242 (1986).

[32] Z. Gasyna, L. Andrews, and P. N. Schatz, J. Phys. Chem. **96**, 1525 (1991).

[33] L. Bergomi and T. Jolicoeur, Saclay preprint 93-119 (1993) (unpublished).

[34] S. Krummacher, M. Biermann, M. Neeb, A. Liebsch, and W. Eberhardt, Phys. Rev. B, 48, 8424 (1993).

[35] R. W. Lof, M. A. van Veenendaal, B. Koopmans, H. T. Jonkman, and G. A. Sawatzky, Phys. Rev. Lett. **68**, 3924 (1992).

[36] O. Gunnarsson, D. Rainer, and G. Zwicknagl, in *Clusters and Fullerenes*, edited by V. Kumar, T. P. Martin, and E. Tosatti (World Scientific, Singapore, 1993) p. 409.

[37] R. M. Fleming, M. J. Rosseinsky, A. P. Ramirez, D. W. Murphy, J. C. Tully, R. C. Haddon, T. Siegrist, R. Tycko, S. H. Glarum, P. Marsh, G. Dabbagh, S. M. Zahurak, A. V. Makhija, and C. Hampton, Nature **352**, 701 (1992).

[38] M. C. Martin, D. Koller, and L. Mihaly, Phys. Rev. B **47**, 14607 (1993).

[39] X. Wei, S. Jeglinski, O. Paredes, Z. V. Vardeny, D. Moses, V. I. Srdanov, G. D. Stucky, K. C. Khemani and F. Wudl, Sol. Stat. Commun. **85**, 455 (1993).

[40] M. De Seta and F. Evangelisti, Phys. Rev. Lett. **71**, 2477 (1993).

[41] L. Yu *et al.* (private communication).

Table I

n	N_v	original degeneracy	2^{nd} order shift $\frac{\Delta^{(2)}}{g^2\hbar\omega}$	residual degeneracy	excit. energy $\frac{E^{(2)}-E^{(2)}_{ground}}{\hbar\omega}$	$^{2S+1}\Re$
1	0	$3(\times 2)$	-5/4	3	0	^{2}P
$(S=\frac{1}{2})$	1	$15(\times 2)$	-2	7	$1-\frac{3}{4}g^2$	^{2}F
			-7/8	5	$1+\frac{3}{8}g^2$	^{2}D
			-1/8	3	$1+\frac{9}{8}g^2$	^{2}P
2	0	6	-5	1	0	^{1}S
$(S=0)$			-11/4	5	$\frac{9}{4}g^2$	^{1}D
	1	30	-5	5	1	^{1}D
			-17/4	9	$1+\frac{3}{4}g^2$	^{1}G
			-11/4	7	$1+\frac{9}{4}g^2$	^{1}F
			-13/8	5	$1+\frac{27}{8}g^2$	^{1}D
			-7/8	3	$1+\frac{33}{8}g^2$	^{1}P
			-1/2	1	$1+9g^2$	^{1}S
2	0	$3(\times 3)$	-5/4	3	0	^{3}P
$(S=1)$	1	$15(\times 3)$	-2	7	$1-\frac{3}{4}g^2$	^{3}F
			-7/8	5	$1+\frac{3}{8}g^2$	^{3}D
			-1/8	3	$1+\frac{9}{8}g^2$	^{3}P
3	0	$8(\times 2)$	-15/4	3	0	^{2}P
$(S=\frac{1}{2})$			-9/4	5	$\frac{3}{2}g^2$	^{2}D
	1	$40(\times 2)$	-9/2	7	$1-\frac{3}{4}g^2$	^{2}F
			-15/4	9	1	^{2}G
			-15/4	5	1	^{2}D
			-21/8	3	$1+\frac{9}{8}g^2$	^{2}P
			-9/4	7	$1+\frac{3}{2}g^2$	^{2}F
			-9/8	5	$1+\frac{11}{8}g^2$	^{2}D
			-3/8	3	$1+\frac{27}{8}g^2$	^{2}P
			0	1	$1+\frac{15}{4}g^2$	^{2}S
3	0	$1(\times 4)$	0	1	0	^{4}S
$(S=\frac{3}{2})$	1	$5(\times 4)$	0	5	1	^{4}D

TABLE I. Analytical expressions of energy shifts and excitation energies for the electron-vibron coupling of a single H_g mode, for low-spin and high-spin states, to second order in the coupling constant g.

Table II

H_g mode	Exp.Energy (cm^{-1}) [6]	coupling g_k [18] [10] [9]	excitation energy $E_{fin} - E_{ground}$ (cm^{-1})			L_{fin} (sym.)
1	270.0	0.33 0.33 0.54	248	248	212	3 $(T_{2u} \oplus G_u)$
			281	281	299	2 (H_u)
			303	303	357	1 (T_{1u})
2	430.5	0.37 0.15 0.40	387	423	380	3 $(T_{2u} \oplus G_u)$
			452	434	456	2 (H_u)
			496	441	507	1 (T_{1u})
3	708.5	0.20 0.12 0.23	687	701	679	3 $(T_{2u} \oplus G_u)$
			719	712	723	2 (H_u)
			741	719	752	1 (T_{1u})
4	772.5	0.19 0.00 0.30	751	773	722	3 $(T_{2u} \oplus G_u)$
			783	773	798	2 (H_u)
			805	773	849	1 (T_{1u})
5	1099.0	0.16 0.23 0.09	1077	1055	1092	3 $(T_{2u} \oplus G_u)$
			1110	1121	1103	2 (H_u)
			1132	1164	1110	1 (T_{1u})
6	1248.0	0.25 0.00 0.15	1190	1248	1226	3 $(T_{2u} \oplus G_u)$
			1277	1248	1259	2 (H_u)
			1335	1248	1281	1 (T_{1u})
7	1426.0	0.37 0.48 0.30	1281	1179	1332	3 $(T_{2u} \oplus G_u)$
			1499	1549	1473	2 (H_u)
			1644	1796	1568	1 (T_{1u})
8	1575.0	0.37 0.26 0.24	1415	1495	1510	3 $(T_{2u} \oplus G_u)$
			1655	1615	1608	2 (H_u)
			1815	1695	1673	1 (T_{1u})

TABLE II. Vibronic excitation spectrum for the eight H_g modes. Three different sets of coupling constants used in the perturbative expressions of Table I. The relations [9] between the coupling strength g and the electron-

phonon coupling $\lambda/N(\epsilon_F)$ (See Ref. [18]) are for H_g modes $g^2 = \frac{6}{5}\lambda/N(\epsilon_F)/\hbar\omega$, and for A_g modes $g^2 = 3\lambda/N(\epsilon_F)/\hbar\omega$.

Table III

mode	U_1	U_2	U_3
A_g	$-2E^{JT}_{0\ k}$	$E^{JT}_{0\ k}$	$4E^{JT}_{0\ k}$
H_g	$-5E^{JT}_{2\ k}$	$10E^{JT}_{2\ k}$	$-5E^{JT}_{2\ k}$

TABLE III. Analytical expressions for single mode pair energies (low-spin states) to second order in the corresponding coupling constants g_k.

Table IV

	Exp.Energy (cm^{-1}) [6]	coupling g_k [18]	Ground state energy shift (meV) n=1	n=2	n=3
$E_{A_g,1}$	493.0	0.38	-5	-18	-27
$E_{A_g,2}$	1468.5	0.39	-14	-54	-81
$E_{H_g,3}$	270.0	0.33	-5	-18	-14
$E_{H_g,4}$	430.5	0.37	-9	-36	-27
$E_{H_g,5}$	708.5	0.20	-5	-18	-14
$E_{H_g,6}$	772.5	0.19	-5	-18	-14
$E_{H_g,7}$	1099.0	0.16	-5	-18	-14
$E_{H_g,8}$	1248.0	0.25	-12	-48	-36
$E_{H_g,9}$	1426.0	0.37	-30	-120	-90
$E_{H_g,10}$	1575.0	0.37	-33	-132	-99
E_{A_g}			-18	-72	-108
E_{H_g}			-102	-408	-306
E_{tot}			-120	-480	-414
U_{n,A_g}			-36	18	72
U_{n,H_g}			-204	408	-204
$U_{n,tot}$			-240	426	-132

TABLE IV. Dynamical JT ground state energy shifts due to each mode, their total, and the pair energies U_n. Results are accurate to second order in the coupling constants g_k.

Figure 1: Exact (solid line) and perturbative energies (dashed line) for n=1, one coupled H_g mode of frequency ω. The straight lines correspond to second order perturbation theory for the N_v=0 and N_v=1 multiplets.

Figure 2: Exact (solid line) and perturbative energies (dashed line) for n=2, one coupled H_g mode of frequency ω. The perturbative lines correspond to the N_v=0 and the lowest three multiplets of N_v=1.

Figure 3: Exact (solid line) and perturbative energies (dashed line) for n=2, one coupled H_g mode of frequency ω. The perturbative lines correspond to the N_v=0 and the lowest three multiplets of N_v=1. The second order coupling does not split the L=4 and L=2 levels in the N_v=1 multiplet, while the exact theory finds they actually do separate. The next excited level (of species P) is also drawn to show its crossing of the initially lower D level

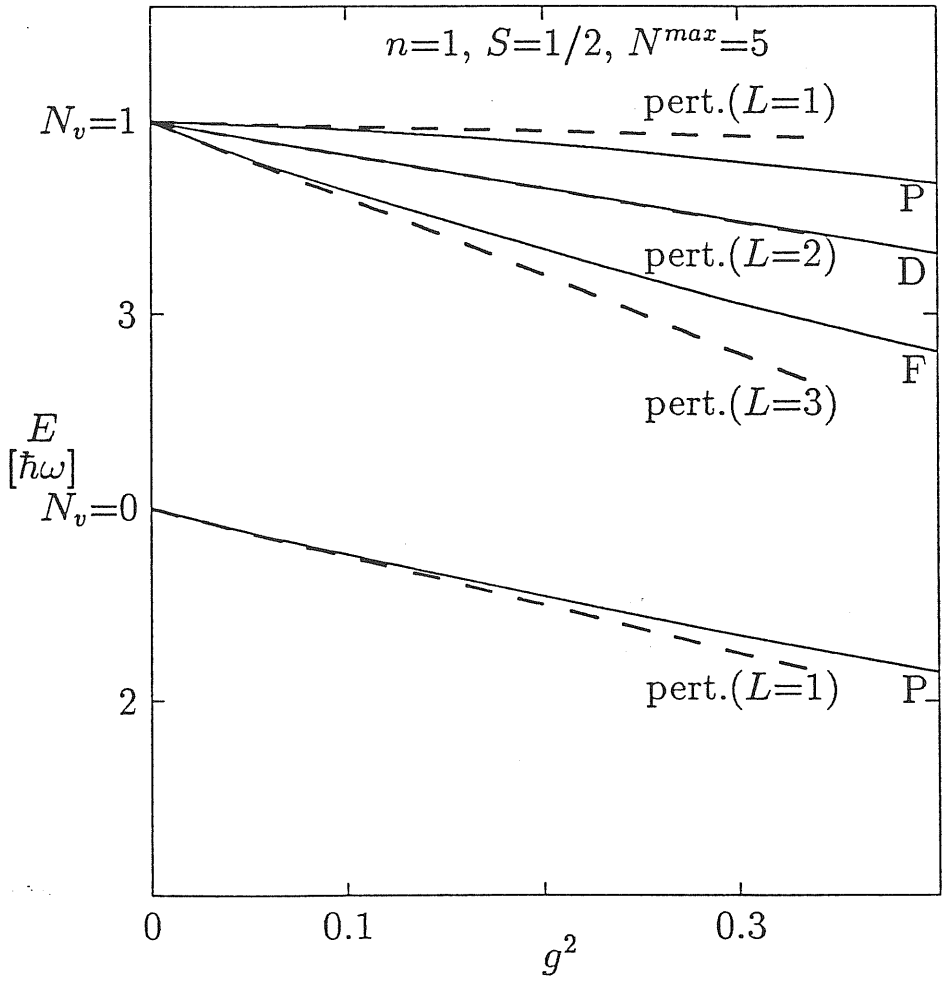

Manini, Tosatti, Anderbach [Part II]

fig. 1

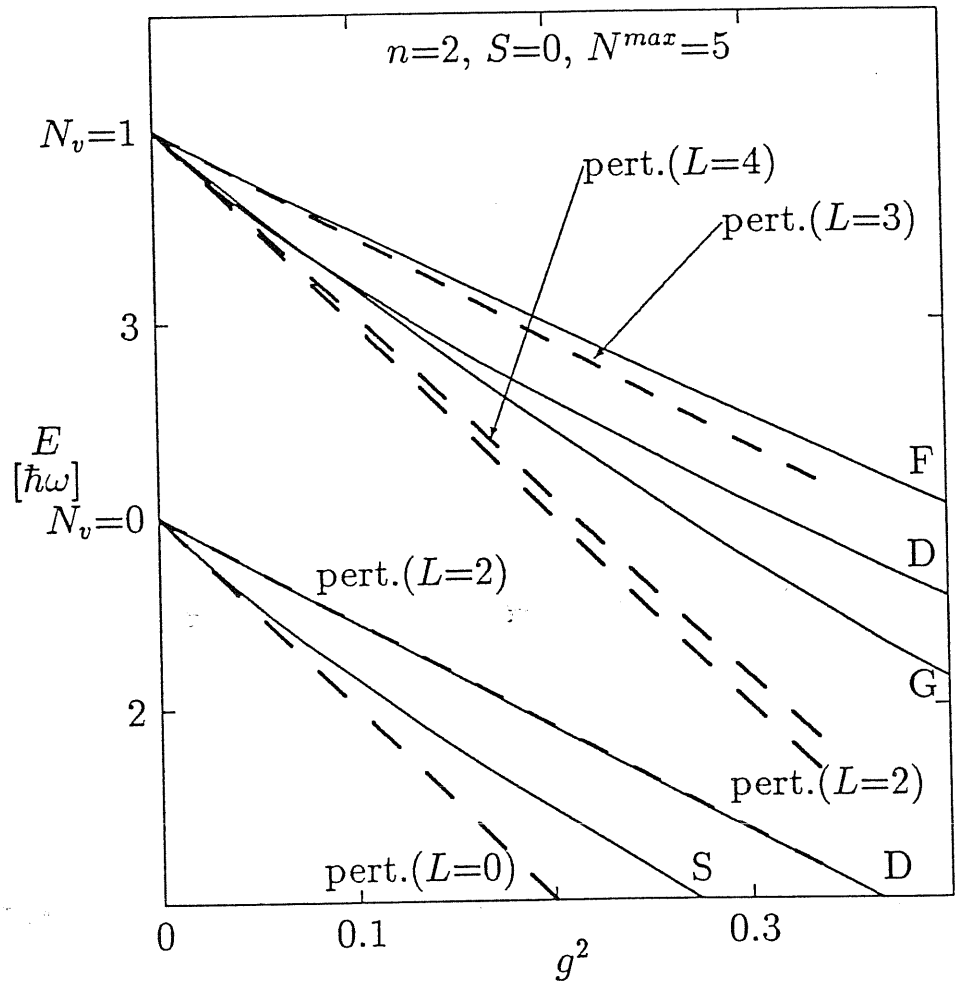

Manini, Tosatti, Anerbach [Part II]

fig 2

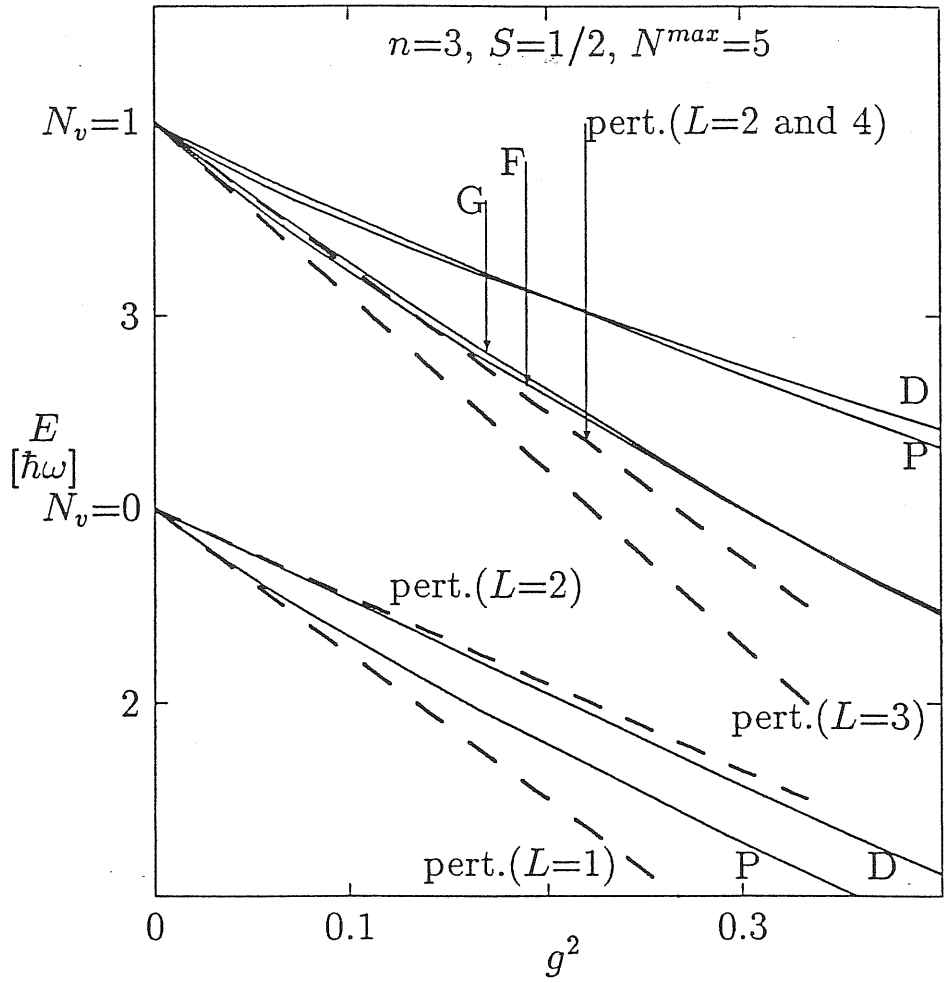

Manini Tosatti Anderlach [Part II]

fig. 3